



A high-resolution synthesis dataset for multistressor analyses along the U.S. West Coast

Esther G. Kennedy^{1, 2}, Meghan Zulian^{1, 2}, Sara L. Hamilton^{2, 3}, Tessa M. Hill^{1, 2}, Manuel Delgado², Carina R. Fish^{1, 2}, Brian Gaylord^{2, 4}, Kristy J. Kroeker⁵, Hannah M. Palmer^{1, 2}, Aurora M. Ricart^{6, 7}, Eric Sanford^{2, 4}, Ana K. Spalding^{8, 9}, Melissa Ward¹⁰, Guadalupe Carrasco¹¹, Meredith Elliott¹², Genece V. Grisby¹, Evan Harris¹, Jaime Jahncke¹², Catherine N. Rocheleau¹, Sebastian Westerink¹³, Maddie I. Wilmot¹

¹Department of Earth and Planetary Sciences, University of California Davis, Davis, CA, USA

²Bodega Marine Laboratory, University of California Davis, Bodega Bay, CA, USA

10 ³Oregon Kelp Alliance, Port Orford, OR, USA

⁴Department of Evolution and Ecology, University of California Davis, Davis, CA, USA

⁵Department of Ecology and Evolutionary Biology, University of California Santa Cruz, Santa Cruz, CA, USA

⁶Institut de Ciències del Mar, ICM-CSIC, Barcelona, Spain

⁷Bigelow Laboratory for Ocean Sciences, East Boothbay, ME, USA

15 ⁸Oregon State University, Corvallis, OR, USA

⁹Smithsonian Tropical Research Institute, Panama City, Panama

¹⁰Coastal and Marine Institute, San Diego State University, San Diego, CA, USA

¹¹Department of Biology, Sonoma State University, Rohnert Park, CA, USA

¹²Point Blue Conservation Science, Petaluma, CA, USA

20 ¹³Department of Land, Air and Water Resources, University of California Davis, Davis, CA, USA

Correspondence to: Esther G. Kennedy (egkennedy@ucdavis.edu)

Abstract. The global trends of ocean warming, deoxygenation, and acidification are not easily extrapolated to coastal environments. Local factors, including intricate hydrodynamics, high primary productivity, freshwater inputs, and pollution, can exacerbate or attenuate global trends and produce complex mosaics of physiologically stressful conditions for organisms. In the California Current System (CCS), oceanographic monitoring programs document some of this complexity; however, data fragmentation and limited data availability constrain our understanding of when and where stressful coastal conditions manifest. Here, we undertake a large data synthesis to compile, format, and quality-control publicly available oceanographic data to create an accessible database for coastal CCS climate risk mapping, available at the National Centers for Environmental Information (Accession 0277984) under the DOI 10.25921/2vve-fh39 (Kennedy et al., 2023). With this synthesis, we combine publicly available observations and data contributed by the author team from synoptic oceanographic cruises, autonomous sensors, and shore samples with relevance to coastal ocean acidification and hypoxia (OAH) risk. This large-scale compilation includes 13.7 million observations from 67 sources. Here, we discuss the quality and composition of the synthesized dataset, the spatial and temporal distribution of available data, and examples of potential analyses. This dataset will provide a valuable tool for assessing regional and local climate risk, evaluating the efficacy and completeness of CCS monitoring efforts, and investigating spatiotemporal scales of coastal oceanographic variability.



1 Introduction

Anthropogenic carbon dioxide (CO₂) emissions are causing dramatic ocean warming, acidification, and deoxygenation (Caldiera and Wickett, 2003; Doney et al., 2009; Doney 2010; Levitus et al., 2012). Interactions among these stressors can compound the severity of each, often synergistically reducing growth, metabolism, and survival of marine organisms across
40 diverse taxa (e.g., Byrne and Przeslawski, 2013; Gobler and Baumann, 2016). Multiparameter extreme events are increasingly common and destructive (Burger et al., 2013; Breitburg et al., 2015). However, global ocean trends may be masked, modified, or overshadowed in coastal ecosystems by combinations of complex local oceanographic processes, effluent from coastal settlements and agriculture, freshwater sources, and diverse and highly productive ecological communities (Doney 2010; Bauer et al., 2013; Duarte et al., 2013; Woodson et al., 2019). Despite thorough documentation
45 of global ocean responses to anthropogenic forcing, understanding more localized conditions in coastal environments, such as the California Current System (CCS), remains an active area of research. Improved understanding of spatiotemporal patterns of warming, deoxygenation, and acidification is key to informing climate resilience and adaptation planning for and by the diverse peoples and ecological communities that depend on the coastal CCS (Field and Francis, 2006; Hodgson et al., 2018; IPCC 2019; Weisberg et al., 2020; Ward et al., 2022).

50

The CCS is an upwelling ecosystem where seasonal winds transport cold, low-oxygen, high-CO₂ waters from depth up to nearshore surface environments (e.g. Hickey, 1979; Huyer, 1983; Chavez and Messié, 2009). Upwelling intensity varies across small spatial and temporal scales and is typically concentrated in the spring and early summer (Hickey, 1979; Marchesiello et al., 2003; García-Reyes and Largier, 2012; Jacox et al., 2018; Cheresh and Fiechter, 2020). During
55 upwelling, minimal values of seasonal dissolved oxygen and carbonate chemistry parameters such as pH are naturally close to biologically significant thresholds, making organisms in the CCS particularly vulnerable to ocean acidification and hypoxia (OAH) events (e.g., Chan et al., 2008; Connolly et al., 2010; Feely et al., 2008; Gruber et al., 2012; Low et al., 2021; Kekuewa et al., 2022). Local adaptation to high environmental variability may provide some ecological resilience (e.g., Sanford and Kelly, 2011; Kelly and Hofmann., 2013; Donham et al., 2023), but widespread die-offs are already a
60 feature of some OAH events (e.g., Grantham et al., 2004; Barton et al., 2015). The CCS is also vulnerable to warming and heatwaves (Cavole et al., 2016; Frölicher and Laufkötter, 2018; Rogers-Bennett and Catton, 2019; Sanford et al., 2019; Fumo et al., 2020; Cheung and Frölicher, 2020). When extreme temperatures interact with low pH and low oxygen conditions, they can compound the vulnerability of organisms to environmental stressors (e.g., Kroeker et al., 2013; Swiney et al., 2017; Bednaršek et al., 2019; Howard et al., 2020b; Sunday et al., 2021). The balance between local upwelling
65 intensity, warming-induced stratification, and both oceanic and terrestrial influences creates a spatiotemporal mosaic of coastal ocean conditions which, while previously acknowledged and documented (e.g., Feely et al., 2016, Chan et al., 2017; Cheresh and Fiechter, 2020), remains incompletely described.



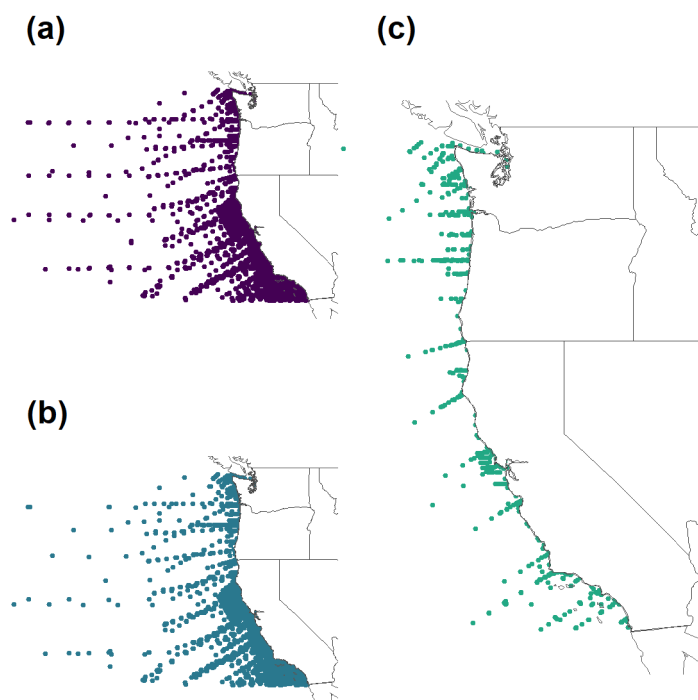
As a result of the connections between upwelling, low oxygen, and acidification events, models predict the CCS's
70 vulnerability to extreme events will increase as climate change progresses (Gruber et al., 2012; Bakun et al., 2015). Relative
to a preindustrial baseline, anthropogenic forcing has shoaled corrosive and hypoxic conditions by more than 50 m (Bograd
et al., 2008; Feely et al., 2008; Chan et al., 2008; Gruber et al., 2012). Modeled projections of the CCS suggest that pH levels
are declining sufficiently swiftly that by 2035 the range of annual variability may no longer overlap with conditions present
in the 2010s, while the calcium carbonate mineral aragonite could be perennially undersaturated at 100 m depth by 2045
75 (Hauri et al., 2013; Marshall et al., 2017). Meanwhile, nearshore dissolved oxygen concentrations are expected to decline by
10-20 $\mu\text{mol kg}^{-1}$ by the end of the century (Siedlecki et al., 2021). Upwelling-favorable winds may intensify under future
warming (Sydeman et al., 2014; Bakun et al., 2015; Wang et al., 2015); although this effect may be counteracted in some
locations by increased stratification of seawater layers (Howard et al., 2020a; Siedlecki et al., 2021) or in areas where wind-
driven upwelling is not the dominant process (García-Reyes and Largier, 2010). These competing forces might enhance the
80 disparities between climate hot spots and refugia, underlining the importance of gathering and analyzing climate data with
high spatiotemporal resolution.

Despite recognition of the complexity of CCS coastal climate stress, successfully capturing mesoscale, sub-seasonal, and
very nearshore patterns of OAH and warming remains challenging. One impediment to unraveling this complexity is the
85 decentralized and non-standardized nature of much OAH monitoring in the CCS, undertaken by governmental, non-profit,
and academic centers with varying methodologies and approaches to data accessibility (Taylor-Burns et al., 2020). Further,
existing synthesis datasets are not optimized for simultaneous analysis of nearshore warming, deoxygenation, and
acidification risks (e.g., Hofmann et al., 2011; Sharp et al., 2022). While several excellent databases compile place-specific
biogeochemical data, such as CeNCOOS and SCCOOS (Terrill et al., 2006; Ruhl et al., 2021), they often are limited
90 regionally, provide access to only a single parameter at a time, lack key datasets, or do not require standard data formats or
quality assurance/quality control (QA/QC) methods (Weisberg et al., 2020).

A deliberate synthesis of OAH-relevant datasets with standardized formatting and quality control maximizes our ability to
explore, map, and resolve coastal climate stress on sub-regional scales (Bushinsky et al., 2019; Chan et al., 2019). Here, we
95 present the Multistressor Observations of Coastal Hypoxia and Acidification (MOCHA) synthesis, the highest resolution
OAH-relevant U.S. West Coast dataset to date. MOCHA is a compilation of published nearshore temperature, dissolved
oxygen, and carbonate chemistry-relevant datasets for the CCS newly available archived at the National Centers for
Environmental Information (NCEI, <https://doi.org/10.25921/2vve-fh39>) along with associated metadata and quality
assurance in adherence with the FAIR principles (Wilkinson et al., 2016; Kennedy et al., 2023). We source published data
100 from oceanographic cruises, buoys, moorings, and shore samples as well as previously unpublished observations contributed
by the author team and present them in a formatted, quality-controlled, downloadable database for easy access and analysis
(Fig. 1). While this dataset is not exhaustive, it both highlights real disparities in oceanographic monitoring intensity and



provides future investigators the opportunity to compare and integrate their own datasets. This synthesis provides an important tool for scientists across disciplines and coastal decision-makers to investigate spatiotemporal variation in marine climate risk from OAH events and warming, evaluate the efficacy and completeness of CCS monitoring efforts, link oceanographic conditions to coastal social or socio-economic considerations across large geographic ranges, evaluate spatial management zones such as aquaculture sites and Marine Protected Areas, and pursue other questions of interest to coastal communities.



110 **Figure 1: All individual locations for temperature (a), dissolved oxygen (b), and carbonate-system (c) observations included in this synthesis along the U.S. West Coast. These figures overstate the useful spatial density of the data, as many individual locations have only been sampled once, but highlight the limited scale of available carbonate-system observations relative to more commonly assessed parameters like temperature and dissolved oxygen.**

2. Methods

115 2.1 Data Sources and Types

This project compiled published and publicly available data, as well as data contributed by the author team, including multiparameter OAH-relevant observations from shipboard discrete water samples, *in-situ* autonomous sensors, and shore-collected datasets from along the U.S. West Coast. We primarily sourced multiparameter data through existing public data portals, such as NCEI and literature searches, prioritizing datasets that included carbonate-system or dissolved oxygen



120 observations in addition to temperature. When available alongside our target parameters, we also incorporated published
chlorophyll and nutrient concentrations. In all cases, we took the published or publicly hosted data as our starting point,
rather than asking for the unprocessed data from the original investigators, then applied additional quality-control measures
described in Sect. 2.4. We have limited this publication to data collected before 2020, but we will continue to incorporate
new observations according to the methods outlined below, where possible, and will periodically make updated versions of
125 this synthesis dataset publicly available at NCEI (<https://doi.org/10.25921/2vve-fh39>; Kennedy et al., 2023).

The data in this synthesis comes from a wide array of observational methods and instruments. We screened carbonate-system
datasets before incorporating them following the discussions of method reliability summarized in Martz et al., (2015). The
carbonate-system observational methods included in this synthesis dataset are: discrete seawater samples of pH, total
130 alkalinity (TA), and dissolved inorganic carbon (DIC) (all preserved at the time of collection and analyzed in a lab with
established techniques; e.g., Dickson et al., 2007); pH observations from ion-sensitive field-effect transistor-based
autonomous sensors (e.g., Honeywell Durafet; Martz et al., 2010) or spectrophotometric sensors (e.g., SAMI-pH; Lai et al.,
2018); and pCO₂ observations from autonomous equilibrium-based spectrophotometric sensors (e.g., SAMI-CO₂; Schar et
al., 2009). We did not include pH measured on glass electrode sensors, due to known issues with precision (Martz et al.,
135 2010). We discarded any dissolved oxygen and carbonate-system datasets that lacked accompanying temperature data, as
accurate observations of both parameters require simultaneous temperature readings (Dickson et al., 2007). Data collection
methods are available for all parameters except temperature and salinity and have been simplified into four groups:
“discrete”, for bottle-collected samples analyzed in a laboratory, “CTD” for observations from ship-side profiling devices,
“autonomous sensors”, for stationary instruments collecting data at pre-programmed intervals, and “handheld sensors” for
140 observations collected in the field via a glass-electrode probe. The specific instruments associated with each data source are
available in the Metadata Table archived at NCEI, Accession 0277984 (Kennedy et al., 2023).

2.2 Formatting

After identifying a dataset of interest, we downloaded all available processed data and metadata, including descriptive
papers, primary investigator information, project and instrument descriptions, and the original source of the data. Each
145 dataset was assigned a unique identifying number to ensure that every data point could be quickly associated with its parent
data source and metadata (Table 1). For all datasets, we retained a copy of the original published data. We manipulated all
original data into a comma-separated file with minimal alterations - typically limited to eliminating extra header rows and
streamlining column names - before transferring datasets into R or Python for further formatting to ensure that all
manipulations were trackable.

150

This synthesis dataset is structured such that each row represents a set of oceanographic observations from a shared time,
depth, location, and data source. For easy filtering, we included a “collection method” column that classified each dataset as



one of four types: “cruise” for ship-collected samples, “mooring” for autonomous instruments attached to buoys, “intertidal/subtidal autonomous sensor” for shore- or diver-accessed autonomous sensors, and “intertidal/subtidal hand
 155 collected” for water samples collected by hand from a dock or the shore. We also assigned each observation a habitat type, labeling observations as “estuarine” if they were collected within semi-restricted lagoons and bays (e.g., Humboldt Bay), or “oceanic” otherwise. We recorded measured variables, data types, and data quality in adjacent columns.

For a full description of included parameters, refer to the detailed metadata table archived at NCEI (Kennedy et al., 2023).

160 We retained all directly measured chemical oceanographic observations as we incorporated each dataset, converted observations to standard units if necessary, and mapped them directly to our corresponding synthesis dataset columns. We did not retain published data calculated from algorithms, such as TA extrapolated from salinity measurements, nor any calculated carbonate system variables, regardless of whether the source publication included such data. While we note that published data may have been summarized or filtered by the initial investigators, we did not further summarize or filter data
 165 before including it in this compilation except for the Ocean Observatories Initiative (OOI) datasets, discussed below.

ID	Dataset	Primary location	Sampling scheme	Habitat	Parameters	Depths
1	SBC LTER: Reference: Sea-surface water temperature, Santa Barbara Harbor, Santa Barbara, CA, USA	Santa Barbara, CA	Intertidal/Subtidal hand collection	Oceanic	Temperature	0 m
2	National Data Buoy Center Station BDXC1 Bodega Head, CA	Bodega Head, CA	Mooring	Oceanic	Temperature Salinity Chlorophyll	0 m
3	SBC LTER: Ocean: Time-series: Mid-water SeaFET and CO ₂ system chemistry at Alegria (ALE)	Santa Barbara, CA	Mooring	Oceanic	Temperature Salinity pH TA	3 m
5	Chemical and hydrographic profile measurements during the 2016 West Coast Ocean Acidification Cruise (WCOA2016, May 5 to June 7,	West Coast of the U.S.	Cruise	Oceanic	Temperature Salinity pH DIC TA	2 m to 2503 m



	2016)						DO Chl Nutrients	
6	National Data Buoy Center Station 46025 Santa Monica Basin, CA	Channel Islands, CA	Mooring	Oceanic	Temperature Salinity	1 m		
7	National Data Buoy Center Station 46217 Anacapa Passage, CA	Channel Islands, CA	Mooring	Oceanic	Temperature	0.46 m		
8	National Data Buoy Center Station 46053 Channel Islands, CA	Channel Islands, CA	Mooring	Oceanic	Temperature Salinity	1 m		
9	National Data Buoy Center Station TDPC1 Trinidad, CA	Eureka, CA	Mooring	Oceanic	Temperature Salinity DO Chl	3 m		
10	National Data Buoy Center Station FPXC1 Fort Point, CA	Fort Point, San Francisco Bay, CA	Mooring	Estuarine	Temperature Salinity Chl	0 m		
11	National Data Buoy Center Station 46221 Santa Monica Bay, CA	Santa Monica Bay, CA	Mooring	Oceanic	Temperature	0.46 m		
12	National Data Buoy Center Station 46235 Imperial Beach, CA	Imperial Beach, CA	Mooring	Oceanic	Temperature	0.46 m		
14	National Data Buoy Center Station 46251 Santa Cruz Basin, CA	Santa Cruz Basin, CA	Mooring	Oceanic	Temperature	0.46 m		
15	National Data Buoy Center Station ICAC1 Santa Monica Pier, CA	Santa Monica, CA	Mooring	Oceanic	Temperature	10.3 m		
16	National Data Buoy Center Station PRYC1	Point Reyes, CA	Mooring	Oceanic	Temperature	1.5 m		



	Point Reyes, CA					
17	National Data Buoy Center Station HBXC1 Humboldt Bay Pier, CA	Humboldt Bay, CA	Intertidal/Subtidal sensor deployment	Estuarine	Temperature Salinity DO Chl	0 m
18	National Data Buoy Center Station MBXC1 Morro Bay BM1 T Pier, CA	Morro Bay, CA	Mooring	Estuarine	Temperature Salinity DO Chl	0 m
19	National Data Buoy Center Station MLSC1 Moss Landing, CA	Moss Landing, CA	Mooring	Oceanic	Temperature Salinity DO	0 m
20	National Data Buoy Center Station MTYC1 Monterey Bay, CA	Monterey, CA	Mooring	Oceanic	Temperature Salinity DO Chl	2.1 m
21	Chemical and hydrographic profile measurements during the 2013 West Coast Ocean Acidification Cruise (WCOA2013, August 3–29, 2013)	West Coast of the U.S.	Cruise	Oceanic	Temperature Salinity pH DIC TA DO Chl Nutrients	2 m to 2530 m
22	Chemical and hydrographic measurements during the 2012 West Coast Ocean Acidification Cruise (WCOA2012, September 4–17, 2012)	West Coast of the U.S.	Cruise	Oceanic	Temperature Salinity DIC TA DO Chl Nutrients	1.7 m to 2963 m



23	Chemical and hydrographic profile measurements during the 2011 West Coast Ocean Acidification Cruise (WCOA2011, August 12–30, 2011)	West Coast of the U.S.	Cruise	Oceanic	Temperature Salinity pH DIC TA DO Chl Nutrients	1.4 m to 2800 m
24	Dissolved inorganic carbon, alkalinity, temperature, salinity and other variables collected from discrete sample and profile observations using Alkalinity titrator, CTD and other instruments from WECOMA in the U.S. West Coast California Current System from 2007-05-11 to 2007-06-14 (NCEI Accession 0083685)	West Coast of the U.S.	Cruise	Oceanic	Temperature Salinity DIC TA DO Nutrients	3.2 m to 4199 m
25	California Cooperative Oceanic Fisheries Investigations (CalCOFI) Bottle Database: Oceanographic data collected from chemical analyses of seawater samples (1949 - present)	California	Cruise	Oceanic	Temperature Salinity DIC TA DO Chl Nutrients	0 m to 5165 m
26	Applied California Current Ecosystem Studies Partnership Discrete Carbonate Chemistry Observations (2013-2019)	Central California	Cruise	Oceanic	Temperature Salinity pH TA DO	1 m to 500 m
27	UC Davis Coastal Ocean Acidification Dataset	West Coast	Intertidal/Subtidal hand collection	Oceanic	Temperature Salinity	0 m



					pH DIC TA DO	
28	Bodega Marine Laboratory Weekly Horseshoe Cove Shore Samples	Bodega Marine Laboratory, CA	Intertidal/Subtidal hand collection	Oceanic	Temperature Salinity pH DIC TA DO	0 m
30	SBC LTER: Ocean: Time- series: Mid-water SeaFET pH and CO ₂ system chemistry with surface and bottom Dissolved Oxygen at Arroyo Quemado Reef (ARQ), 2012-2017	Arroyo Quemado	Mooring	Oceanic	Temperature Salinity pH TA DO	4 m
31	SBC LTER: Ocean: Time- series: Mid-water SeaFET pH and CO ₂ system chemistry with surface and bottom Dissolved Oxygen at Mohawk Reef (MKO), 2012 - 2017	Mohawk Reef	Mooring	Oceanic	Temperature Salinity pH TA DO	4 m
32	SBC LTER: Ocean: Time- series: Mid-water SeaFET pH and CO ₂ system chemistry with surface and bottom Dissolved Oxygen at Santa Barbara Harbor/Stearns Wharf (SBH), 2012-2017	Santa Barbara Harbor/Stearns Wharf	Mooring	Oceanic	Temperature Salinity pH TA DO	4 m



33	Ocean Margin Ecosystems Group for Acidification Studies (OMEGAS) Project: Acclimation and adaptation to ocean acidification of key ecosystem components in the California Current System	West Coast	Intertidal/Subtidal sensor deployment	Oceanic	Temperature pH	1 m
34	EAGER Project: Initiation of a pH/pCO ₂ -sensing mooring platform on the Oregon coast	Oregon	Mooring	Oceanic	Temperature pCO ₂	70 m
35	pCO ₂ pH salinity and temperature collected off the coast of Oregon USA by a SAMI-CO ₂ - Shelf Break and NH10	Oregon	Mooring	Oceanic	Temperature Salinity pH pCO ₂	2 m and 120 m
36	SBC LTER: pH time series: Water-sample pH and CO ₂ system chemistry	California	Cruise	Oceanic	Temperature Salinity pH DIC TA	0 m to 15 m
37	Bodega Marine Reserve Monthly Shore Samples	Bodega Marine Reserve, CA	Intertidal/Subtidal hand collection	Oceanic	Temperature Salinity pH DIC TA DO	0 m
38	Tomales Estuary Line Bottles	Tomales Bay, CA	Cruise	Estuarine	Temperature Salinity pH DIC TA DO Chl	0 m to 9 m



39	California Coastal Seagrass Project	California	Intertidal/Subtidal sensor deployment	Varies by site	Temperature Salinity pH TA DO	0 m and 2 m
40	California kelp forest tidal FET sites	California	Intertidal/Subtidal sensor deployment	Oceanic	Temperature pH DO	10 m to 13 m
41	Dissolved inorganic carbon (DIC), total alkalinity (TA), temperature, salinity, oxygen, and nutrient data collected from discrete profile measurements during the National Oceanic and Atmospheric Administration Harmful Algal Blooms (NOAA HABs) program cruise SH1709 (EXPOCODE 332220170918) in Pacific Northwest marine waters on NOAA Ship Bell M. Shimada from 2017-09-18 to 2017-09-28 (NCEI Accession number 0208230)	Washington	Cruise	Oceanic	Temperature Salinity DIC TA DO Nutrients	2 m to 2890 m
42	Dissolved inorganic carbon, total alkalinity, nutrients, and other variables collected from profile and discrete observations using CTD, Niskin bottle, and other instruments from R/V New Horizon and R/V Robert Gordon Sproul in the U.S. West Coast for calibration and validation of California Current	Southern California Bight	Cruise	Oceanic	Temperature Salinity DIC TA DO Chl Nutrients	2 m to 3038 m



	Ecosystem (CCE) Moorings from 2009-12-15 to 2015-04-29 (NCEI Accession 0146024)					
43	High-resolution ocean and atmosphere pCO ₂ time-series measurements from mooring CCE1_122W_33N in the North Pacific Ocean from 2008-11-11 to 2020-06-11 (NCEI Accession 0144245)	Point Conception, CA	Mooring	Oceanic	Temperature Salinity pH pCO ₂ fCO ₂ DO	0 m
44	High-resolution ocean and atmosphere pCO ₂ time-series measurements from Mooring CCE2_121W_34N in the North Pacific Ocean from 2010-01-17 to 2021-06-16 (NCEI Accession 0084099)	Point Conception, CA	Mooring	Oceanic	Temperature Salinity pH pCO ₂ fCO ₂ DO	0 m
45	CeNCOOS in situ water monitoring data at Trinidad Head, California	Trinidad, CA	Intertidal/Subtidal sensor deployment	Oceanic	Temperature Salinity DO Chl	0 m
46	SFSU EOS YSI Raw data	Tiburon Peninsula, CA	Intertidal/Subtidal sensor	Estuarine	Temperature Salinity Chl	1 m
47	CeNCOOS in situ Water monitoring data at the Santa Cruz municipal wharf	Santa Cruz, CA	Intertidal/Subtidal sensor deployment	Oceanic	Temperature Salinity DO	1 m



					Chl	
49	San Francisco Estuary Institute and the Aquatic Science Center Regional Monitoring Program for Water Quality in San Francisco Bay	San Francisco Bay, CA	Cruise	Estuarine	Temperature Salinity DO Chl	0 m to 88 m
50	West Coast Estuary Data: Santa Monica Bay (15 m) autonomous monitoring coastal acidification data and Santa Monica Bay (60 m) autonomous monitoring coastal acidification data	Santa Monica	Mooring	Oceanic	Temperature Salinity pH pCO ₂ DO	15 m and 60 m
51	West Coast Estuary Data: San Francisco Bay (surface) autonomous monitoring coastal acidification data and San Francisco Bay (deep water mooring) autonomous monitoring coastal acidification data	SF Bay	Mooring	Estuarine	Temperature Salinity pH DO Chl	1 m and 17 m
52	Dissolved inorganic carbon, alkalinity, temperature, salinity, and nutrient data for validation measurements for moored ocean acidification time-series observations of on the Cha Ba mooring off La Push, Washington (May 2011-October 2014)	LaPush, WA	Cruise	Oceanic	Temperature Salinity DIC TA Nutrients	1.5 m to 101 m
53	Morro Bay BM1 T-Pier (NOAA Station MBXC1)	Morro Bay, CA	Mooring	Estuarine	Temperature Salinity	1 m



					pH DO Chl	
54	Morro Bay BS1 Station	Morro Bay, CA	Mooring	Estuarine	Temperature Salinity pH DO Chl	1 m
55	High-resolution ocean and atmosphere pCO ₂ time-series measurements from mooring WA_125W_47N in the North Pacific Ocean (NCEI Accession 0115322)	Cape Elizabeth, WA	Mooring	Oceanic	Temperature Salinity pH pCO ₂ fCO ₂ DO	1 m
56	Stillwater Cove TidalFET	Carmel, CA	Intertidal/Subtidal sensor deployment	Oceanic	Temperature Salinity pH DO	1 m
57	National Data Buoy Center Station 46211 Grays Harbor, WA	Grays Harbor, WA	Mooring	Oceanic	Temperature	0.46 m
58	National Data Buoy Center Station NEAW1 - 9443090 Neah Bay, WA	Neah Bay, WA	Mooring	Estuarine	Temperature	1.19 m
59	National Data Buoy Center Station CECC1 - 9419750 Crescent City, CA	Crescent City, CA	Intertidal/Subtidal sensor deployment	Oceanic	Temperature	1.3 m
60	National Data Buoy Center Station 46237 San Francisco, CA	San Francisco, CA	Mooring	Oceanic	Temperature	0.46 m
61	National Data Buoy Center Station 46240 Cabrillo Point, Monterey Bay,	Monterey Bay, CA	Mooring	Oceanic	Temperature	1 m



	CA - 158 Monterey Bay, CA					
62	National Data Buoy Center Station PORO3 Port Orford, OR	Port Orford, OR	Mooring	Oceanic	Temperature	1.3 m
63	National Data Buoy Center Station CHAO3 Charleston, OR	Charleston, OR	Mooring	Estuarine	Temperature	2 m
64	High-resolution ocean and atmosphere pCO ₂ time-series measurements from mooring CB-06_125W_43N in the North Pacific Ocean (NCEI Accession 0190840)	Coos Bay, OR	Mooring	Oceanic	Temperature Salinity pH pCO ₂ fCO ₂ DO Chl	0 m
65	High-resolution ocean and atmosphere pCO ₂ time-series measurements from mooring NH10_124W_44N in the North Pacific Ocean (NCEI Accession 0157247)	Newport, OR	Mooring	Oceanic	Temperature Salinity pH pCO ₂ fCO ₂ DO Chl	1.7 m
66	Ocean Observatories Initiative (OOI) Washington and Oregon Inshore and Shelf Moorings	Washington and Oregon	Mooring	Oceanic	Temperature pH DO	0 m, 7 m, and 87 m
67	Trinidad Head Line CTD Hydrography	Northern California	Cruise	Oceanic	Temperature Salinity pH DO	1 m to 545 m



68	Spatially gridded cross-shelf hydrographic sections and monthly climatologies from shipboard survey data collected along the Newport Hydrographic Line, 1997–2021	Central Oregon	Cruise	Oceanic	Temperature Salinity DO	0 m to 3000m
69	Oceanographic Data Across Oregon's Marine Reserves	Oregon	Mooring	Oceanic	Temperature DO	15 m
70	CMOP: Physical and biogeochemical observation stations in the Columbia River estuary (Saturn-02)	Columbia River Estuary, OR	Mooring	Estuarine	Temperature Salinity DO	6 m and 35 m
71	Monthly cross-shore transects of biogeochemical properties in La Jolla, CA	Southern CA	Cruise	Oceanic	Temperature Salinity pH DIC TA DO Nutrients	0 m to 40 m

Table 1: Overview of the included data sources in the MOCHA compilation. The origins of all the included datasets in this compilation are fully described and cited in the Metadata Table available at NCEI (<https://doi.org/10.25921/2vve-flh39>, Kennedy et al., 2023). Detailed discussions of the following datasets have been previously published: 5 (Feely et al., 2008); 21-24, 26 (Feely et al., 2016); 25 (Bograd et al., 2003); 26 (Davis et al., 2018); 33 (Chan et al., 2017); 38 (Hollarsmith et al., 2020); 39 (Ricart et al., 2021); 40 (Kroeker et al., 2023); 49 (Salop and Herrmann, 2019); 50 and 51 (Rosenau et al., 2021); 56 (Donham et al., 2022); 66 (Trowbridge et al., 2019); 67 (Bjorkstedt and Peterson, 2015); 68 (Risien et al., 2022); 69 (Barth et al., 2021); 70 (Baptista et al., 2015); and 71 (Kekuewa et al., 2022).

2.3 Ocean Observatories Initiative (OOI) Datasets

The Washington and Oregon OOI data included millions of observations of temperature, salinity, dissolved oxygen, pH, and pCO₂ at sub-minute resolutions. The size of these datasets required us to aggregate the data to daily mean values before incorporation into the larger synthesis dataset. We filtered raw OOI with input from the OOI staff to remove outlying and unreliable data, grouped the remaining data by day, aggregated to daily mean values, then quality-controlled the aggregated data a second time according to the methods described in Sect. 2.4.



Because much of the publicly available OOI data had not been previously quality controlled, we contacted OOI staff for their guidance on initially filtering the raw data before aggregation. They provided extensive code developed by the sensor manufacturers and OOI staff to identify erroneous pH and DO data from the raw publicly available streams, available at <https://github.com/oceanobservatories/ooi-data-explorations/tree/master/python>. OOI staff also provided access to discrete sample analyses taken at the sensor moorings to further ground-truth sensor readings. We only retained data for aggregation if it 1) passed through the manufacturer's code, 2) had discrete samples associated with the beginning and end of that sensor's deployment, 3) the daily mean sensor values for dissolved oxygen and pH on the day of discrete sampling were within 20 $\mu\text{mol/kg}$ of the discrete sample dissolved oxygen and/or 0.05 pH units, and 4) displayed reasonable DO/pH concentrations and variance in those concentrations over time. We eliminated all DO data prior to 2018 based on advice of OOI staff because the DO sensors prior did not have adequate biofouling control. We then aggregated these data into daily mean values before formatting and quality controlling them as normal.

2.4 Quality Control

After formatting individual datasets, we checked all observations to standardize quality across data sets and avoid using questionable data points in future analyses. Our QA/QC methods drew from a combination of the publishing authors' notes, plots of the data, and expert knowledge of the CCS. Incoming quality-control notes associated with each data source ranged widely, though most datasets that did include quality information followed the Quality Assurance/Quality Control of Real-Time Oceanographic Data (QARTOD) system, which assigns flags based on internal instrument checks, data reasonableness, and collection method (Bushnell 2018). Using available existing QA/QC information and our further quality control investigations, we categorized each data point as one of three confidence levels: 1 for "plausible and reliable" data, 2 for data that we had not assessed yet, and 3 for "low quality or unreliable" data. We flagged all data the publishing authors had listed as unreliable with a 3. Regardless of published notes, we assigned all other observations a flag of 2 before additional evaluation by our project team.

Given the diversity of the datasets and projects this synthesis draws from, we examined each dataset individually using a combination of plots tailored to maximize our ability to identify and evaluate anomalies in that dataset's specific oceanographic and spatiotemporal context. Given that this synthesis sources mostly published data, we erred towards retaining data as "plausible", rather than following a more stringent flagging philosophy. We recommend that investigators perform additional QC with the MOCHA dataset targeted towards their project requirements. Common quality control plotting techniques included property-property plots of temperature, salinity, dissolved oxygen, pH, total alkalinity, and dissolved inorganic carbon against one another; single-parameter time series from sensor and long-running datasets; and map views and oceanographic cross sections of synoptic cruise data. We examined questionable data through as many different views as possible, such as examining apparent outliers in a temperature-salinity property-property plot individually in their respective time series, to ensure that we were not trimming real or plausible observations. When possible, we further



215 evaluated suspicious observations against other datasets collected nearby. We discussed all data flagging decisions with at least three project members. After this focused quality control, all observations not flagged as “low quality or unreliable” (3) were upgraded to our “plausible and reliable” flag (1). All subsequent mapping and analysis with the observed oceanographic values used only “plausible and reliable” data.

2.5 Example Subset: Daily Data

220 High-resolution (sub-daily observations) autonomous sensors are an important component of this synthesis dataset, but the data they produce comes with significant computational costs. Furthermore, variability on the scales of hours or minutes captured by such high-resolution records is less comparable to lower-resolution datasets such as those collected over quarterly or annual synoptic oceanographic cruises. To evaluate the spatiotemporal extent of our data coverage, seasonal patterns, and relationships between observed parameters, we aggregated the dataset to daily mean values for each location, depth, and data source. We dropped all questionable data (i.e. data flagged with a “3” QA/QC code) before creating this
225 summary dataset to ensure that unreliable data did not influence averages. This reduced the total number of observations from 13.7 million to 1.2 million. We used this summary dataset in all following analyses that do not explicitly cite “original data.” We have included the code necessary to reproduce this summary dataset from the published data compilation in our public code repository (https://github.com/egkennedy/DSP_public_code).

2.6 Additional Carbonate System Calculations

230 To maximize the OAH information available in our daily summarized dataset, we calculated the full carbonate system parameters for all discrete samples that included at least two high-quality observations of primary variables of the carbonate system (pH, TA, DIC, or pCO₂) in addition to high-quality, co-occurring temperature and salinity measurements. These calculated parameters can be reproduced using the code in our public code repository (https://github.com/egkennedy/DSP_public_code). We used the R package “seacarb” (Gattuso et al., 2018) for all carbonate
235 system calculations and used constants appropriate for the temperature and salinity as recommended by Dickson et al. (2007). In cases where more than two carbonate system parameters were available, we prioritized TA-DIC pairs following Dickson (2010), then TA-pH pairs, then DIC-pH pairs. When applicable for mapping and time series analyses, measured and calculated carbonate system observations were concatenated, with measured data prioritized in all overdetermined systems. All references to an analysis of “original” data and all discussions of the distribution of observations only include directly
240 measured variables; however, the oceanographic relationships discussed in Sect 3.5 and shown in Figs. 3, 5, and 6 include these additional calculated observations.



3 Results and Discussion

3.1 Overall Data Totals

This synthesis dataset includes observations from 67 individual data sources organized across 13.7 million rows and 41
 245 columns. This includes 24.1 million unique measurements, with 13.2 million temperature, 3.6 million salinity, 3.3 million
 DO, 2.1 million pH, 1.2 million chlorophyll, 561,000 nutrient, 113,000 pCO₂, 10,400 TA, and 8,500 DIC measurements.
 While we prioritized multiparameter datasets for this effort, our synthesis also includes several temperature-only, high-
 resolution records to fill specific project needs. Summarizing the data by day for each dataset, location, and depth provides a
 clearer picture of the availability of multiparameter data by muting the outsized influence of high-resolution sensors. Of the
 250 1.2 million daily averaged observations, just 104,000 are temperature-only.

Data totals across dissolved oxygen and carbonate-system observations varied substantially by observational method.
 Autonomous sensors are the most common observational method in the original dataset with 5 million individual
 measurements, versus 226,000 individual discrete measurements, 193,000 CTD measurements, and 828 handheld field
 255 measurements. Across data aggregated by day, autonomous sensors are still the most common, with 643,000 individual daily
 averaged parameter measurements, versus 223,000 discrete, 192,000 CTD, and 816 handheld sensor observations. For
 evaluating the spatiotemporal coverage of carbonate-system observations, we calculated an additional 4,599 daily pH
 observations from paired discrete samples of two other primary carbonate system parameters, equal to 3.1% of the total
 directly measured daily pH observations (Table 2). The calculated pH observations were included in our analysis of the
 260 spatiotemporal extent of available OAH data discussed in Sect 3.3 and the oceanographic relationships discussed in Sect.
 3.5.

Parameter	Collection Method	Daily Total Observations	Reliability Rate
DO	discrete	8363	99.70%
	autonomous sensor	564020	92.40%
	CTD	128961	99.90%
	handheld sensor	816	98.70%
pH	discrete	4912	98.70%
	autonomous sensor	78895	88.70%
	CTD	63404	100%

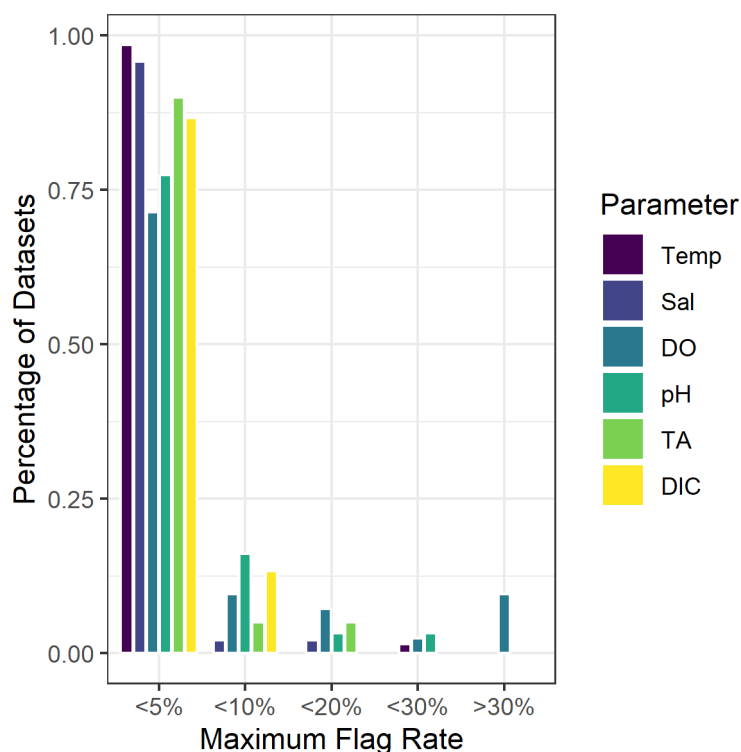


	calculated	4599	
DIC	discrete	8363	99.10%
TA	discrete	9908	98.70%

265 **Table 2: Overview of parameter observation methods, total number of daily observations (grouped by data source, location, and depth), and the reliability rates. Autonomous sensors are associated with slightly lower reliability rates due to periods of sensor bio fouling or malfunction.**

3.2 Flagging and Reliability

270 The amount of original data flagged as unreliable varied substantially by dataset, parameter, and observation method, but was typically low (Fig. 2). As the bulk of the data in this synthesis product was previously published and had undergone some preliminary QA/QC prior to our incorporation, high reliability rates were expected. Of the dozens of datasets contributing temperature and salinity observations, only one dataset each had a parameter flag rate above 5%. Flag rates above 10% were uncommon for all parameters across all datasets, and completely absent for TA and DIC observations. For pH and DO, flag rates within datasets were above 10% for 3 and 8 datasets, respectively. These high rates of “unreliable” data were caused by either 1) clear periods of autonomous sensor malfunction 2) observational methods described by the publishing authors as unreliable, or 3) more rarely, slightly higher QA/QC standards applied to data that had not been previously screened and published. The vulnerability of autonomous sensors to periods of biofouling or sensor malfunction contributed to higher flag rates relative to other methods, but all four methods were largely reliable (Table 2). Across all datasets, 99.8% temperature, 96.8% salinity, 93.1% DO, 89.1% pH, 99.1% DIC, and 98.7% TA observations were considered “reliable or plausible”. Across all individual observations, 97.3% are classified as reliable.



280 **Figure 2: The rate of unreliable (“flagged”) observations varied by parameter and dataset, but was generally low, especially for**
temperature (Temp) and salinity (Sal) observations. All datasets that included dissolved oxygen (DO) observations with a >30%
flag rates used measurement methods described by the original publishers as “not quantitative”. Flag rates between 10% and 30%
285 **were uncommon, but reflected occasional periods of fouling or equipment malfunction in high resolution autonomous sensor**
datasets or, in rare cases, more stringent standards applied to datasets that had not been previously published and initially quality
controlled.

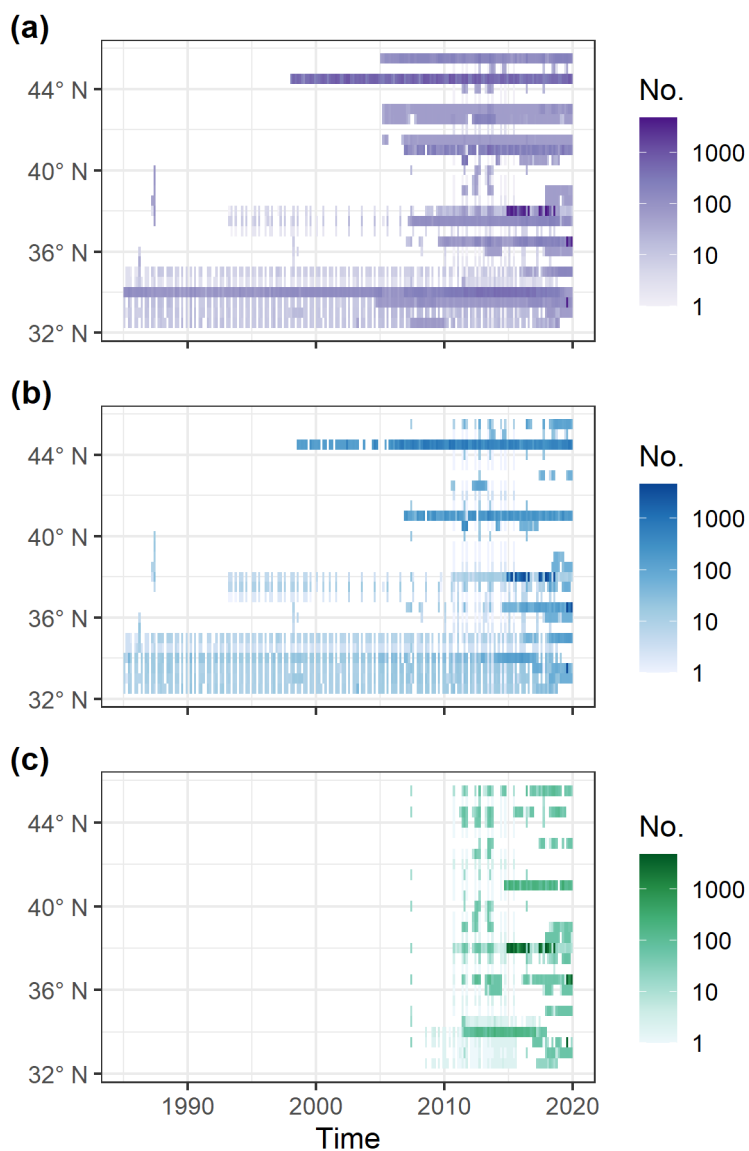
3.3 Spatiotemporal Data Distribution

This dataset spans the U.S. West Coast and reflects the spatiotemporal bias of observational records. Observations are more common in nearshore, near-surface environments and exhibit greater sampling effort in recent years. Fifty-seven percent of daily observations were collected within 50 km of shore and 37% within 50 m of the surface. Eighty-six percent of all daily observations were collected after 1990. Carbonate-system observations are especially skewed toward recent years, with no observations in this compilation (of pH, TA, DIC, or pCO₂) prior to 2006. By contrast, temperature, salinity, and dissolved oxygen records are common after 1980.

The spatiotemporal coverage of our dataset is highly variable, though improving through time. Mapping the density of surface, nearshore (<25 m depth and <50 km from shore) observations along the coastline through time highlights the influence of dense coastal human populations and major research institutions (Fig. 3). By contrast, the region between Point Arena, California and central Oregon is much less densely observed and lost considerable oceanographic monitoring



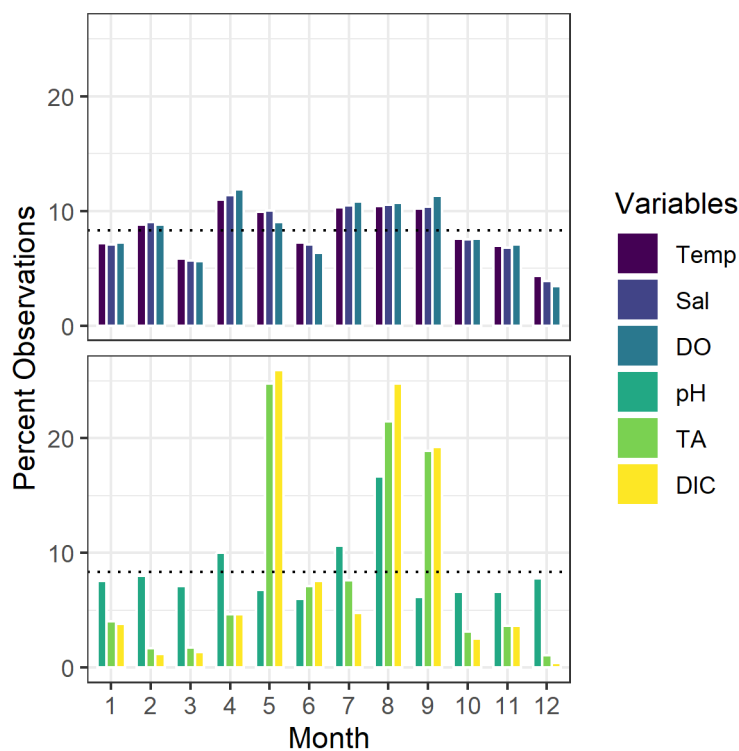
300 capacity between 2015 and 2020. Temperature and dissolved oxygen measurements have the most extensive coverage, but are sparse outside of Southern California before 2000. Carbonate system records, here shown by both measured and calculated pH observations, are rare in all years north of 39° N. Overall, this data compilation demonstrates large spatial and temporal data gaps, which limit our ability to resolve rapid changes in ocean acidification, hypoxia, or warming risk or to contextualize current carbonate-system and dissolved oxygen conditions with respect to the recent past.



305 **Figure 3: The number of nearshore (< 50 km from shore), near-surface (< 25 m) observations within a two-month period for temperature (a), dissolved oxygen (b), and pH (c) along the coast. The full carbonate-system observational density is captured by pH alone. Spatial data coverage was best across all parameters between 2010 and 2015. Since then, dissolved oxygen and pH measurements have become less common along the coast despite increasing awareness of the risks of nearshore acidification and hypoxia events.**



310 The intra-annual distribution of the daily data is more complex than the interannual distribution (Fig. 4). Temperature, salinity, and dissolved oxygen records are common throughout the year, but have distinct peaks in abundance in April, May, and July through November. Carbonate system records are more patchy temporally. Nearly 50% of all TA and DIC observations were taken in May or August, with an additional 19% of observations from September, reflecting the sampling months of the NOAA West Coast Ocean Acidification Cruises (Feely et al., 2016). Between October and April, no single
315 month includes more than 8% of DIC observations or 5% of TA observations. pH observations are more evenly distributed throughout the year, with all months hosting 6-10.5% of the observations except August, which hosts 16%. The concentration of carbonate-system observations between May and September is particularly concerning, as upwelling season in Central and Southern California starts in earnest in April (García-Reyes and Largier, 2012; Jacox et al., 2018) and at least two carbonate-system parameters must be measured to fully constrain the carbonate system (Dixon et al., 2007), so the
320 observational record may be missing significant low pH, low DO events from the early upwelling season.



325 **Figure 4: The distribution of daily observations by month varies substantially by parameter relative to an equal split (dashed lines). Temperature (Temp) , salinity (Sal), and dissolved oxygen (DO) observations are fairly evenly distributed across seasons, with notable observational peaks in April, July, August, and September. Carbonate system parameters (pH, total alkalinity or TA, and dissolved inorganic carbon or DIC) are more concentrated in the summer months, with nearly all TA and DIC observations occurring in May, August, or September. Of the carbonate-system parameters, only pH observations nearly equitably distributed throughout the year.**



3.5 Data Relationships

This synthesis dataset effectively captures seasonal and regional variability across OAH-relevant parameters (Fig. 5).
330 Median surface, nearshore (<25 m depth and <50 km from shore) temperatures rise in all regions during the spring and
summer months, peaking between July and September. In Washington and Oregon, peak upwelling occurs between June and
August (Bograd et al., 2009; Jacox et al., 2016), which coincides with the period of highest variability and lowest minima for
pH and DO observations captured in this synthesis. In both California regions, seasonal surface data is less consistent with
the expected upwelling patterns. There, peak upwelling occurs between April and June and is weakest south of Point
335 Conception (Bograd et al., 2009; García-Reyes and Largier, 2012; Jacox et al., 2016). Somewhat unexpectedly, the highest
variability and lowest minimum DO and pH observations occur between July and September in both California regions
rather than during the months of expected peak upwelling. This trend may reflect intermittent upwelling into the warmer
summer months or could be capturing high surface respiration as waters warm and invites further investigation. October
through March conditions across all West Coast regions are more poorly sampled, but have less variability, cooler mean
340 temperatures, and higher dissolved oxygen concentrations and pH.

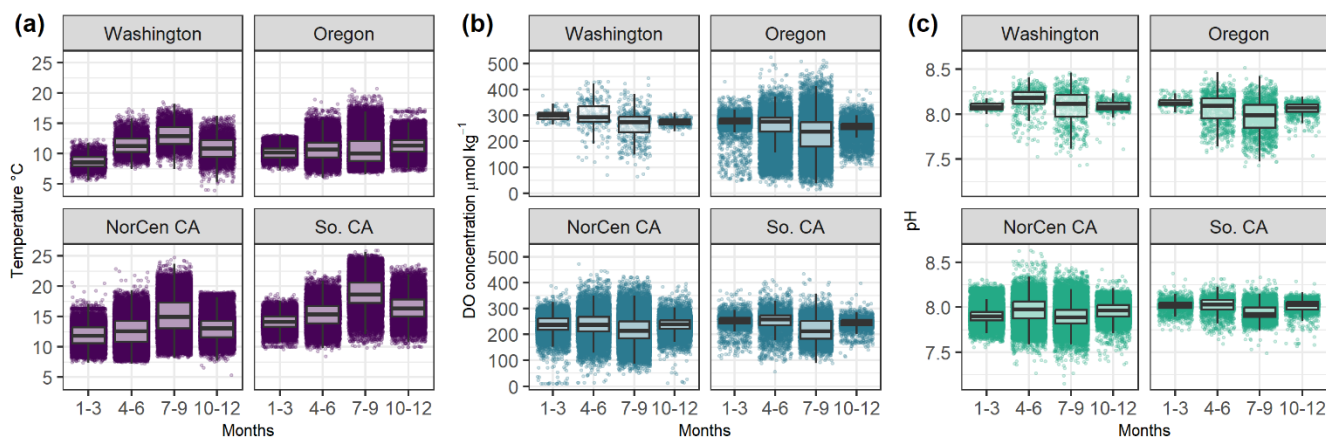
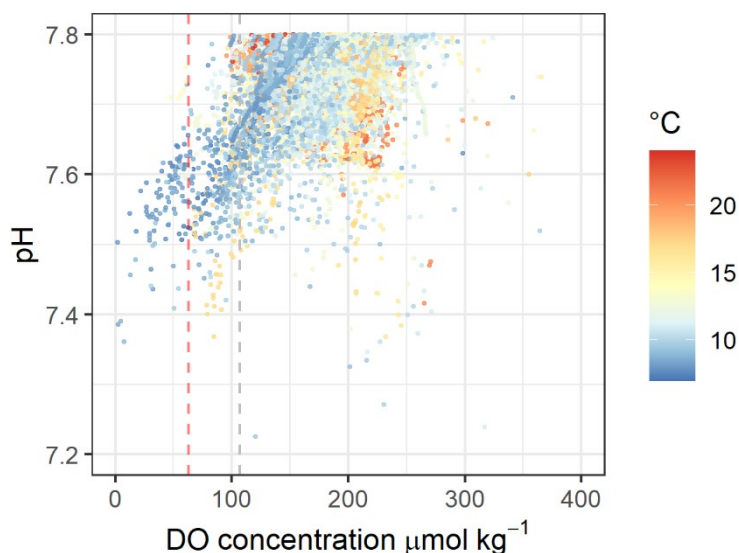


**Figure 5: Nearshore (< 50 km from shore), near-surface (< 25m) observations of temperature (a), dissolved oxygen (DO) (b), and
345 pH (c) capture intra-annual and regional variation. While upwelling, which brings low temperature, low DO, low pH water to the
surface, is most common between April and June, median surface conditions do not reflect this phenomenon due to the episodic
nature of upwelling and high variability in the system. The lowest median DO and pH conditions are found with the highest
temperatures in late summer. Here, California is split into two regions: NorCen CA, spanning the northern border to Point
Conception (34.5 N), and So. CA, from Point Conception to the southern border.**

The relationships between daily measured OAH parameters illustrate the complexity of nearshore oceanographic processes.
350 As expected in an upwelling ecosystem, low surface pH and DO conditions are most frequently associated with low
temperatures, but warmer OAH events still occur (Fig. 6). pH conditions below 7.8 can be stressful for many marine
organisms (e.g., Byrne and Przeslawski, 2013; Gobler and Baumann, 2016; Bednaršek et al., 2021; Kroeker et al, in press)
and have been observed 9,928 times within 50 km of shore and 50 m of the surface (Fig. 6). Of these instances, 99 events are



355 accompanied by DO concentrations below the “coastal hypoxia” threshold of $61 \mu\text{mol kg}^{-1}$ and 548 events have DO
concentrations below the “mild hypoxia” threshold of $107 \mu\text{mol kg}^{-1}$ (Hofmann et al., 2011). An additional 1,765 nearshore,
near-surface observations of DO concentrations below $61 \mu\text{mol kg}^{-1}$ have been recorded without accompanying pH
information. No simultaneous surface observations of DO and pH record coastal hypoxic conditions with pH levels above
7.8. The low pH, low oxygen observations are most common off the Oregon coast during low temperature upwelling events,
but simultaneous low oxygen, low pH conditions are also found occasionally throughout the coast and at a range of
360 temperatures, especially during late summer in semi-restricted estuaries. The few simultaneous observations of DO
concentration and pH suggest that only 1.0% of observations of low pH ($\text{pH} < 7.8$) are accompanied by hypoxic water, while
shallow hypoxic waters are accompanied by low pH conditions 99% of the time. These relationships underscore the
importance of multiparameter OAH observations, the clear need for pH monitoring efforts to catch up with dissolved oxygen
monitoring efforts, and the potential for even shallow waters to experience extreme conditions.



365

Figure 6: Within 50 km of shore and the top 50 m, waters frequently have pH levels below 7.8. These conditions are most likely to be associated with hypoxic ($<61 \mu\text{mol kg}^{-1}$ dissolved oxygen, red line) or mildly hypoxic ($<107 \mu\text{mol kg}^{-1}$ dissolved oxygen, gray line) conditions during upwelling events, which also bring low temperatures. Low pH conditions are also common at a range of temperatures and dissolved oxygen (DO) concentrations.

370

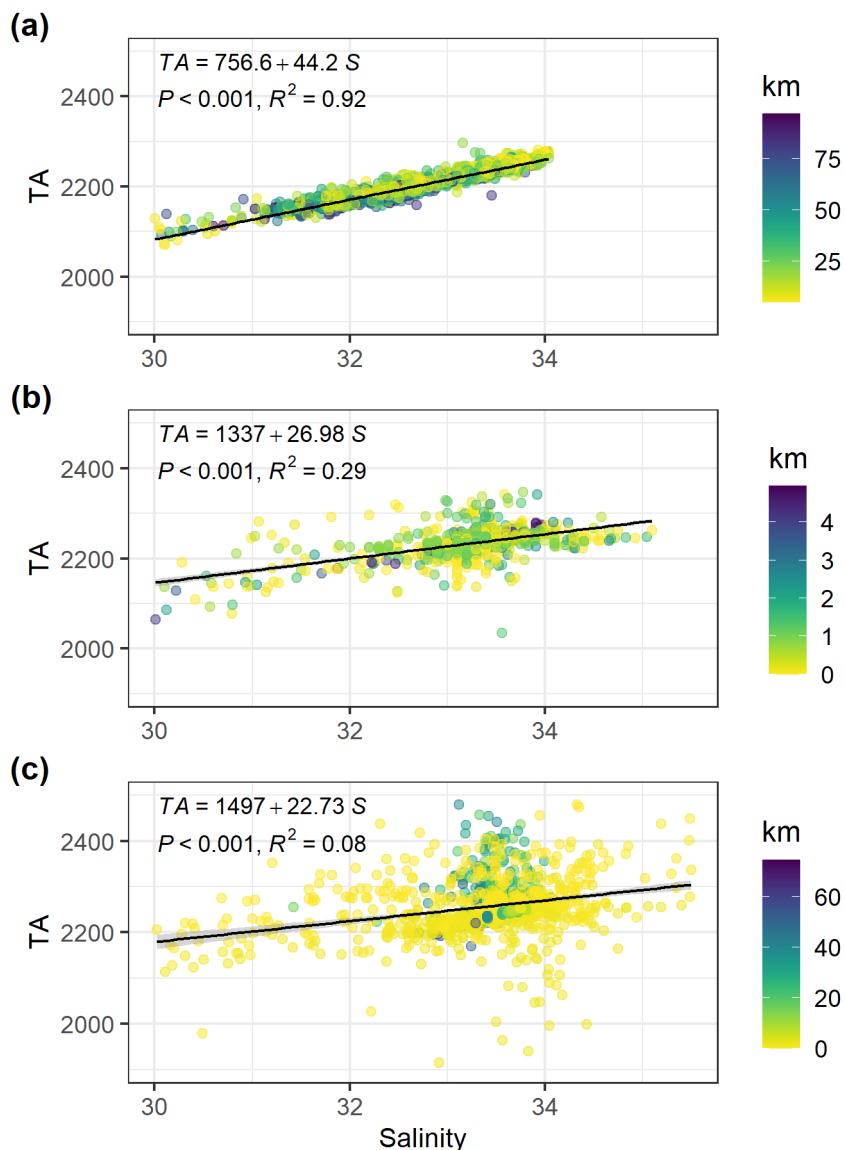
The nearshore, near-surface data in the MOCHA synthesis also highlights the difficulty of developing accurate nearshore algorithms that can predict carbonate-system parameters from other more commonly measured hydrographic variables in coastal ecosystems, even in the absence of large freshwater inputs. The relationship between salinity and TA is regionally dependent and less reliable in nearshore environments and near San Francisco Bay, as has been noted by investigators developing carbonate-system algorithms (Fig. 7; e.g., Alin et al., 2012; Davis et al., 2018). Excluding the San Francisco Bay area, surface TA-salinity relationships are linear and not highly dependent on distance from shore between 5 km and 100 km,
375



though the slope term varies significantly between all regions except Washington and Oregon (Table 3). Within 5 km of shore, TA-salinity relationships in all regions have much weaker fits and have significantly different slopes than the offshore relationships in all regions except Washington. The region around the mouth of San Francisco Bay (between 37.25° N and 38.45° N), TA-salinity relationships are particularly weak, even out to 100 km offshore. The scatter at near-oceanic salinities in the TA-salinity relationship near San Francisco Bay may be a reflection of organic and urban runoff from the Bay Area, as it does not appear to be freshwater-related. While all linear relationships discussed here were significant at the $p < 0.1$ level, the high standard deviations from the TA-salinity regression lines in nearshore environments, and especially within the San Francisco Bay region, translates to 50-200 $\mu\text{mol kg}^{-1}$ of uncertainty in TA concentrations. At depths below 50 m and beyond 100 km from shore, TA-salinity relationships are strong, predictable, and linear, as expected for an open ocean system and successfully leveraged by previous investigators to extrapolate carbonate-system conditions (Alin et al., 2012; Davis et al., 2018; Middelburg et al., 2020). The weakness of coastal TA-salinity relationships underscores the importance of monitoring multiple parameters of the carbonate system.

Region	Offshore relationship	Nearshore relationship
Washington	Slope: 42.29 \pm 0.85 Intercept: 818.30 \pm 27.45 R-squared: 0.83	Slope: 39.38 \pm 4.83 Intercept: 926.28 \pm 152.51 R-squared: 0.74
Oregon	Slope: 42.50 \pm 0.62 Intercept: 811.9 \pm 20.08 R-squared: 0.88	Slope: 36.19 \pm 2.79 Intercept: 1032.11 \pm 91.69 R-squared: 0.55
NorCen CA (except the San Francisco Area)	Slope: 54.70 \pm 0.67 Intercept: 406.22 \pm 22.30 R2: 0.92	Slope: 17.35 \pm 5.37 Intercept: 1654.94 \pm 179.88 R-squared: 0.04
Near San Francisco Bay	Slope: 7.92 \pm 11.98 Intercept: 2011.68 \pm 401.26 R-squared: 0	Slope: 25.43 \pm 2.66 Intercept: 1401.19 \pm 88.59 R-squared: 0.11
Southern California	Slope: 49.77 \pm 1.23 Intercept: 569.06 \pm 41.21 R2: 0.77	Slope: 9.12 \pm 1.79 Intercept: 1933.98 \pm 59.71 R-squared: 0.04

Table 3: Regional surface (<50 m) total alkalinity (TA)-salinity regression relationships for within 5 km of shore versus between 5 and 100 km of shore. All regression relationships are significant ($p < 0.01$). Offshore surface relationships are generally strong except in the San Francisco Bay region, where they are completely non-predictive. Nearshore relationships are weaker than their offshore counterparts in Washington, Oregon, and Southern California and are functionally not predictive in southern CA and the San Francisco Bay region.



395 **Figure 7: Coast-wide near-surface (<50 m) total alkalinity (TA)-salinity relationships from 5-100 km offshore (a), 0-5 km offshore**
(b), and near the mouth of San Francisco Bay (c). Excluding the San Francisco area, TA-salinity relationships between 5 km and
100 km offshore are strong and linear, with small differences between geographic regions. Within 5 km of shore throughout the
Coast and within 100 km of San Francisco Bay (right), the TA-salinity relationships are much less reliable. This limits the utility of
carbonate-system algorithms and emphasizes the need to fully characterize the carbonate-system through simultaneous
400 **measurements of two master parameters to effectively assess nearshore acidification conditions.**

3.6 Dataset Limitations

This data compilation reflects high-quality, publicly available data, and directly contributes to our ability to map coastal temperature, dissolved oxygen, and carbonate-system variation; however, this synthesis also encodes the limitations of our observational record and the differences in data availability, data scales, and data quality. High resolution autonomous



405 sensors provide excellent temporal resolution for a specific location, but are vulnerable to sensor drift, are not often
published with clear calibration records, and are rarely deployed in arrays that fully capture the carbonate system as well as
temperature and dissolved oxygen variability. Conversely, discrete samples and CTD profiles from synoptic cruises provide
extremely high-precision, multiparameter observations with broad spatial resolution, but are less relatable to high-resolution
410 sensors or hand-collected observations from the surf zone. Carbonate-system observation availability has strong seasonal and
spatial bias, with data concentrated in summer months and along coastal population centers. The MOCHA synthesis pulls
these distinct data sources into a single location, but we do not claim to have fully solved the inherent difficulties of
combining data of differing quantity, resolution, and quality into a unified picture of the nearshore CCS.

Additional data streams that provide both spatial and temporal resolution could help bridge some of the divides between
415 quality, quantity, and spatial extent in this synthesis and we acknowledge a few such potential data streams here. The
temperature and dissolved oxygen records do not include CTD casts from most annual fishery-independent surveys, which
could improve spatial resolution at all depths (e.g., Sakuma, 2022). This compilation also excludes some potentially valuable
carbonate system data streams, particularly those focused on pCO₂ measurements. For example, potential additional data
sources include underway pCO₂ records from transiting oceanographic ships or sail drones, pH or pCO₂ records from
420 autonomous gliders (e.g. Chavez et al., 2017), and pCO₂ and DIC records from shore based monitoring systems (e.g., Burke-
o-Lators; Hales et al., 2004; Bandstra et al., 2006). The first would significantly improve the spatial coverage of surface
pCO₂ and could improve seasonal bias, but would not have a significant impact on our ability to resolve the full carbonate
system or to consider deeper water. Glider datasets would similarly improve our spatial coverage while providing additional
information about water column structure. These could represent a valuable expansion to this synthesis, provided calibration
425 records are also available and will likely be included in updates to this synthesis product (Bushinsky et al., 2019). Shore
based monitoring systems recently deployed by the West Coast OOI's will also be valuable expansions to this synthesis and
will also likely be included in an updated product.

4 Conclusions

The CCS is one of the most intensively monitored marine ecosystems in the world, but our ability to accurately resolve the
430 true complexity of coastal climate stress remains limited by data fragmentation, availability, and quality. As interest has
shifted from documentation of the global patterns of acidification and hypoxia to more complex coastal environments, the
CCS has seen an explosion in nearshore (<50 km) and very nearshore (<5 km) monitoring efforts in the last 15 years. This
explosion has included an increase in both surface and subsurface monitoring efforts, though monitoring efforts below 5 m
depth are still much less common than surface observations in very nearshore environments. While this situation is
435 improving, the continued relative paucity of subsurface nearshore measurements is of particular concern given that mildly



hypoxic ($\text{DO} < 107 \text{ } \mu\text{mol kg}^{-1}$) and corrosive conditions have been documented at depths as shallow as 10 m (Kekuewa et al., 2022).

Surprisingly, the U.S. West Coast had especially continuous spatial and temporal coverage of OAH-relevant parameters
440 between 2012 and the beginning of 2015, before a reduction in coverage that lasted through 2020 (Fig. 5). By coincidence, the reduction in dissolved oxygen and carbonate-system monitoring in 2015 coincided with the second half of the marine heatwave known as “the Blob”, which stretched from 2014 through 2016 and was associated with higher surface DO and pH (Bond et al., 2015; Siedlecki et al., 2016; Gentemann et al., 2017). Assessing the interactions of an unprecedented marine heatwave with DO and carbonate-system conditions lies at the heart of multi-stressor risk management; however, our ability
445 to resolve both Blob impacts and its recovery was very limited in Northern California and Oregon by the concurrent contraction in oceanographic monitoring. Although the CCS is well monitored compared to many other parts of the world's oceans, our synthesis here highlights that a patchwork of monitoring projects, often driven by inconsistent funding, has an outsized impact on our ability to utilize that data to understand how the CCS is changing.

450 While increasing interest in coastal OAH monitoring and the availability of autonomous sensors has markedly enhanced CCS data availability, the frequency and footprints of synoptic oceanographic cruises has decreased in the region. Oceanographic cruises provide highly accurate and spatially broad water column measurements that can bridge the gap between the coastal and open-ocean domains and provide regional contexts for local observations. They also provide some of our only observations near remote portions of the coast. However, nearly all routine oceanographic cruises in the CCS
455 have cut back their footprint, sampling frequency, and depth resolution. The Southern California-based CalCOFI cruises extended throughout the CCS during the 1960s, contracted to Southern and Central California by the 1980s, and now only cover the Southern California Bight while also sampling at significantly fewer depths (Bograd et al., 2003). The loss of CalCOFI cruises in Central California has been offset in part by triannual Applied California Current Ecosystem Studies cruises near San Francisco Bay, though these cruises are limited to the continental shelf between 37.3° N and 38.4° N . The
460 NOAA West Coast Ocean Acidification Cruises took place along the entire CCS five times from 2007-2016, but a 2017 cruise only included Washington (Feely et al., 2016; Alin et al., 2019). The shift towards high-resolution, nearshore monitoring is a significant improvement over a wholesale reduction in oceanographic monitoring, but the concurrent erosion of consistent oceanographic cruises means the ability to resolve large-scale regional patterns is being traded for highly-specific understanding of a few select locations.

465 This synthesis dataset provides one of the largest compilations to date of West Coast nearshore acidification and deoxygenation related data. This dataset highlights monitoring gaps, but equally provides opportunities for insight into coastal conditions. With the updated spatiotemporal resolution this effort affords, this dataset offers a wealth of opportunities to investigate questions about coastal oceanography and evaluate localized patterns of marine climate stress. We expect the



470 MOCHA synthesis to also be of use for new projects combining temperature and dissolved oxygen records into species
metabolic indices (e.g., Howard et al., 2020b), for investigating the frequency and interaction of individual and overlapping
ocean acidification and hypoxic events (e.g., Burger et al., 2022), for developing updated carbonate system algorithms more
suited to nearshore environments (e.g., Alin et al., 2012; Davis et al., 2018); and for evaluating the efficacy of spatial
management zones such as Marine Protected Areas (Hamilton et al., in press). By archiving this dataset at the National
475 Centers for Environmental Information (<https://doi.org/10.25921/2vve-fh39>; Kennedy et al., 2023) in an easily manipulated,
consistent format that includes relevant metadata and quality assurance, we provide an important tool for scientists across
ecological, oceanographic, and social disciplines and coastal decision-makers to address the environmental, economic, and
cultural needs of coastal communities.

5 Data Availability

480 The full Multistressor Observations of Coastal Hypoxia and Acidification dataset and detailed metadata tables are publicly
available for download at NCEI as Accession 0277984 with the DOI 10.25921/2vve-fh39 (Kennedy et al., 2023). This data
set is discoverable via the NOAA Ocean Acidification Portal, NCEI Geoportals (<https://www.ncei.noaa.gov/metadata/geoportal/#searchPanel>), and other online discovery tools.

6 Code Availability

485 Code for performing carbonate-system calculations with the formatted dataset, creating a summarized dataset aggregated by
day, and making all included figures is available on GitHub at https://github.com/egkennedy/DSP_public_code.

Competing Interests

The authors declare that they have no conflicts of interest.

Author Contributions

490 After the first four, authors are listed alphabetically in two groups: those who contributed significantly to data acquisition,
interpretation, and overall project direction and those who contributed to data curation. All authors read, edited and approved
of the manuscript. EGK wrote original draft and led data curation and quality control methodology. MZ and SLH provided
substantial manuscript reviews, data curation, and methodology insights. TMH led project conceptualization, funding
acquisition, and supervision, and provided substantial manuscript review. TMH, KJK, JJ, CF, and ME provided previously
495 unpublished data for inclusion. KJK, AKS, BG, ES, and MW contributed to funding acquisition and project



conceptualization. HMP, MW, AMR, GVG, CNR, GC, MD, MIW, EH, and SW provided data curation and sourced new datasets for inclusion.

Acknowledgements

This project received funding from the following sources: California Ocean Protection Council (Hill, Sanford, Gaylord, Kroeker, Spalding) Lenfest Ocean Program (to Hill, Sanford, Gaylord, Kroeker, Spalding), NOAA Ocean Acidification Program (to Hill and Spalding), Packard Foundation (Hill, Sanford, Gaylord, Kroeker), and National Park Service (to Hill) and National Science Foundation (to Kennedy, Grant No. 1734999). We value the partnership of the Applied California Current Ecosystem Studies Partnership (ACCESS, www.accessoceans.org), an ongoing collaboration between Point Blue Conservation Science and Greater Farallones and the Cordell Bank National Marine Sanctuaries to support healthy oceans in north-central California. Brady O'Donnell, Priya Shukla, Lena Capece, Seth Miller, Sarah Merolla, Daphne Bradley and Danielle Lipski assisted with data collection and management. We thank Rachel Carlson and Alyssa Griffin for sharing their advice, expertise, and feedback at key points in the project. We also thank the UC Davis Data Lab for their assistance with data management and coding.

References

- Alin, S. R., Feely, R. A., Dickson, A. G., Hernández-Ayón, J. M., Juraneck, L. W., Ohman, M. D., and Goericke, R.: Robust empirical relationships for estimating the carbonate system in the southern California Current System and application to CalCOFI hydrographic cruise data (2005–2011), *J. of Geophys. Res.: Oceans*, 117, <https://doi.org/10.1029/2011JC007511>, 2012.
- Alin, S. R., Feely, R. A., Newton, J., Trainer, V. L., Adams, N. G., Greeley, D., Curry, B., Herndon, J., and Ostendorf, M. L.: Dissolved inorganic carbon (DIC), total alkalinity (TA), temperature, salinity, oxygen, and nutrient data collected from discrete profile measurements during the National Oceanic and Atmospheric Administration Harmful Algal Blooms (NOAA HABs) program cruise SH1709 (EXPOCODE 3322220170918) in Pacific Northwest marine waters on NOAA Ship Bell M. Shimada from 2017-09-18 to 2017-09-28., NOAA National Centers for Environmental Information, NCEI Accession number 0208230 [data set], <https://doi.org/doi.org/10.25921/3qa5-v720>, 2019.
- Bakun, A., Black, B. A., Bograd, S. J., García-Reyes, M., Miller, A. J., Rykaczewski, R. R., and Sydeman, W. J.: Anticipated effects of climate change on coastal upwelling ecosystems, *Curr. Clim. Change Rep.*, 1, 85–93, <https://doi.org/10.1007/s40641-015-0008-4>, 2015.
- Bandstra, L., Hales, B., and Takahashi, T.: High-frequency measurements of total CO₂: Method development and first oceanographic observations, *Mar. Chem.*, 100, 24–38, <https://doi.org/10.1016/j.marchem.2005.10.009>, 2006.



- 525 Baptista, A. M., Seaton, C., Wilkin, M. P., Riseman, S. F., Needoba, J. A., Maier, D., Turner, P. J., Kärnä, T., Lopez, J. E., Herfort, L., Megler, V. M., McNeil, C., Crump, B. C., Peterson, T. D., Spitz, Y. H., and Simon, H. M.: Infrastructure for collaborative science and societal applications in the Columbia River estuary, *Front. Earth Sci.*, 9, 659–682, <https://doi.org/10.1007/s11707-015-0540-5>, 2015.
- Barth, J. A., Erofeev, A., and Chan, F.: Oceanographic data across Oregon’s marine reserves, Oregon State University, Oregon Department of Fish and Wildlife Marine Resources Program, Newport, OR, 2021.
- 530 Barton, A., Waldbusser, G. G., Feely, R. A., Weisberg, S. B., Newton, J. A., Hales, B., Cudd, S., Eudeline, B., Langdon, C. J., Jefferds, I., King, T., Suhrbier, A., and McLaughlin, K.: Impacts of coastal acidification on the Pacific Northwest shellfish industry and adaptation strategies implemented in response, *Oceanography*, 28, 146–159, 2015.
- Bauer, J. E., Cai, W.-J., Raymond, P. A., Bianchi, T. S., Hopkinson, C. S., and Regnier, P. A. G.: The changing carbon cycle of the coastal ocean, *Nature*, 504, 61–70, <https://doi.org/10.1038/nature12857>, 2013.
- 535 Bednaršek, N., Feely, R. A., Howes, E. L., Hunt, B. P. V., Kessouri, F., León, P., Lischka, S., Maas, A. E., McLaughlin, K., Nezlin, N. P., Sutula, M., and Weisberg, S. B.: Systematic review and meta-analysis toward synthesis of thresholds of ocean acidification impacts on calcifying pteropods and interactions with warming, *Front. Mar. Sci.*, 0, <https://doi.org/10.3389/fmars.2019.00227>, 2019.
- 540 Bednaršek, N., Ambrose, R., Calosi, P., Childers, R. K., Feely, R. A., Litvin, S. Y., Long, W. C., Spicer, J. I., Štrus, J., Taylor, J., Kessouri, F., Roethler, M., Sutula, M., and Weisberg, S. B.: Synthesis of thresholds of ocean acidification impacts on decapods, *Front. Mar. Sci.*, 8, <https://doi.org/10.3389/fmars.2021.651102>, 2021.
- Bjorkstedt, E. P. and Peterson, W. T.: Zooplankton data from high-frequency coastal transects, in: *Coastal Ocean Observing Systems*, Elsevier, 119–142, <https://doi.org/10.1016/B978-0-12-802022-7.00008-0>, 2015.
- 545 Bograd, S. J., Checkley, D. A., and Wooster, W. S.: CalCOFI: a half century of physical, chemical, and biological research in the California Current System, *Deep Sea Res. Part II: Topical Studies in Oceanography*, 50, 2349–2353, [https://doi.org/10.1016/S0967-0645\(03\)00122-X](https://doi.org/10.1016/S0967-0645(03)00122-X), 2003.
- Bograd, S. J., Castro, C. G., Lorenzo, E. D., Palacios, D. M., Bailey, H., Gilly, W., and Chavez, F. P.: Oxygen declines and the shoaling of the hypoxic boundary in the California Current, *Geophys. Res. Lett.*, 35, <https://doi.org/10.1029/2008GL034185>, 2008.
- 550 Bograd, S. J., Schroeder, I., Sarkar, N., Qiu, X., Sydeman, W. J., and Schwing, F. B.: Phenology of coastal upwelling in the California Current, *Geophys. Res. Lett.*, 36, <https://doi.org/10.1029/2008GL035933>, 2009.
- Bond, N. A., Cronin, M. F., Freeland, H., and Mantua, N.: Causes and impacts of the 2014 warm anomaly in the NE Pacific, *Geophys. Res. Lett.*, 42, 3414–3420, <https://doi.org/10.1002/2015GL063306>, 2015.
- 555 Breitbart, D. L., Salisbury, J., Bernhard, J. M., Cai, W.-J., Dupont, S., Doney, S. C., Kroeker, K. J., Levin, L. A., Long, W. C., Milke, L. M., Miller, S. H., Phelan, B., Passow, U., Seibel, B. A., Todgham, A. E., and Tarrant, A. M.: And on top of all that...: Coping with ocean acidification in the midst of many stressors, *Oceanography*, 28, 48–61, 2015.



- Burger, F. A., Terhaar, J., and Frölicher, T. L.: Compound marine heatwaves and ocean acidity extremes, *Nat. Commun.*, 13, 4722, <https://doi.org/10.1038/s41467-022-32120-7>, 2022.
- 560 Bushinsky, S. M., Takeshita, Y., and Williams, N. L.: Observing changes in ocean carbonate chemistry: Our autonomous future, *Curr. Clim. Change Rep.*, 5, 207–220, <https://doi.org/10.1007/s40641-019-00129-8>, 2019.
- Bushnell, M.: Quality Control of Real-Time Water Level Data: The U.S. IOOS® QARTOD Project, *Mar. Technol. Soc. J.*, 52, 13–17, <https://doi.org/10.4031/MTSJ.52.2.2>, 2018.
- Byrne, M. and Przeslawski, R.: Multistressor impacts of warming and acidification of the ocean on marine invertebrates' life
565 histories, *Integr. Comp. Biol.*, 53, 582–596, <https://doi.org/10.1093/icb/ict049>, 2013.
- Caldeira, K. and Wickett, M. E.: Anthropogenic carbon and ocean pH, *Nature*, 425, 365–365, <https://doi.org/10.1038/425365a>, 2003.
- Cavole, L., Demko, A., Diner, R., Giddings, A., Koester, I., Pagniello, C., Paulsen, M.-L., Ramirez-Valdez, A., Schwenck, S., Yen, N., Zill, M., and Franks, P.: Biological impacts of the 2013–2015 warm-water anomaly in the Northeast Pacific:
570 Winners, losers, and the future, *Oceanography*, 29, <https://doi.org/10.5670/oceanog.2016.32>, 2016.
- Chan, F., Barth, J. A., Lubchenco, J., Kirincich, A., Weeks, H., Peterson, W. T., and Menge, B. A.: Emergence of anoxia in the California Current Large Marine Ecosystem, *Science*, 319, 920–920, <https://doi.org/10.1126/science.1149016>, 2008.
- Chan, F., Barth, J. A., Blanchette, C. A., Byrne, R. H., Chavez, F., Cheriton, O., Feely, R. A., Friederich, G., Gaylord, B., Gouhier, T., Hacker, S., Hill, T., Hofmann, G., McManus, M. A., Menge, B. A., Nielsen, K. J., Russell, A., Sanford, E.,
575 Sevadjian, J., and Washburn, L.: Persistent spatial structuring of coastal ocean acidification in the California Current System, *Sci. Rep.*, 7, 1–7, <https://doi.org/10.1038/s41598-017-02777-y>, 2017.
- Chan, F., Barth, J. A., Kroeker, K. J., Lubchenco, J., and Menge, B. A.: The dynamics and impact of ocean acidification and hypoxia: Insights from sustained investigations in the Northern California Current Large Marine Ecosystem, *Oceanography*, 32, 62–71, 2019.
- 580 Chavez, F., Pennington, J. T., Michisaki, R., Blum, M., Chavez, G., Friederich, J., Jones, B., Herlien, R., Kieft, B., Hobson, B., Ren, A., Ryan, J., Sevadjian, J., Wahl, C., Walz, K., Yamahara, K., Friederich, G., and Messié, M.: Climate variability and change: Response of a coastal ocean ecosystem, *Oceanography*, 30, 128–145, <https://doi.org/10.5670/oceanog.2017.429>, 2017.
- Chavez, F. P. and Messié, M.: A comparison of Eastern Boundary Upwelling Ecosystems, *Prog. Oceanogr.*, 83, 80–96,
585 <https://doi.org/10.1016/j.pocean.2009.07.032>, 2009.
- Cheresh, J. and Fiechter, J.: Physical and biogeochemical drivers of alongshore pH and oxygen variability in the California Current System, *Geophys. Res. Lett.*, 47, e2020GL089553, <https://doi.org/10.1029/2020GL089553>, 2020.
- Cheung, W. W. L. and Frölicher, T. L.: Marine heatwaves exacerbate climate change impacts for fisheries in the northeast Pacific, *Sci. Rep.*, 10, 6678, <https://doi.org/10.1038/s41598-020-63650-z>, 2020.
- 590 Connolly, T. P., Hickey, B. M., Geier, S. L., and Cochlan, W. P.: Processes influencing seasonal hypoxia in the northern California Current System, *J. Geophys. Res.: Oceans*, 115, <https://doi.org/10.1029/2009JC005283>, 2010.



- Davis, C. V., Hewett, K., Hill, T. M., Largier, J. L., Gaylord, B., and Jahncke, J.: Reconstructing aragonite saturation state based on an empirical relationship for Northern California, *Estuaries Coast.*, 41, 2056–2069, <https://doi.org/10.1007/s12237-018-0372-0>, 2018.
- 595 Dickson, A. G.: The carbon dioxide system in seawater: Equilibrium chemistry and measurements, in: *Guide to best practices for ocean acidification research and data reporting*, 17–40, 2010.
- Doney, S. C.: The growing human footprint on coastal and open-ocean biogeochemistry, *Science*, 328, 1512–1516, <https://doi.org/10.1126/science.1185198>, 2010.
- Doney, S. C., Fabry, V. J., Feely, R. A., and Kleypas, J. A.: Ocean acidification: The other CO₂ Problem, *Ann. Rev. of Mar. Sci.*, 1, 169–192, <https://doi.org/10.1146/annurev.marine.010908.163834>, 2009.
- 600 Donham, E. M., Strobe, L. T., Hamilton, S. L., and Kroeker, K. J.: Coupled changes in pH, temperature, and dissolved oxygen impact the physiology and ecology of herbivorous kelp forest grazers, *Glob. Change. Biol.*, 28, 3023–3039, <https://doi.org/10.1111/gcb.16125>, 2022.
- Donham, E. M., Flores, I., Hooper, A., O’Brien, E., Vylet, K., Takeshita, Y., Freiwald, J., and Kroeker, K. J.: Population-specific vulnerability to ocean change in a multistressor environment, *Sci. Adv.*, 9, eade2365, <https://doi.org/10.1126/sciadv.ade2365>, 2023.
- 605 Duarte, C. M., Hendriks, I. E., Moore, T. S., Olsen, Y. S., Steckbauer, A., Ramajo, L., Carstensen, J., Trotter, J. A., and McCulloch, M.: Is ocean acidification an open-ocean syndrome? Understanding anthropogenic impacts on seawater pH, *Estuaries Coast.*, 36, 221–236, <https://doi.org/10.1007/s12237-013-9594-3>, 2013.
- 610 Feely, R. A., Sabine, C. L., Hernandez-Ayon, J. M., Ianson, D., and Hales, B.: Evidence for upwelling of corrosive “acidified” water onto the continental shelf, *Science*, 320, 1490–1492, <https://doi.org/10.1126/science.1155676>, 2008.
- Feely, R. A., Alin, S. R., Carter, B., Bednaršek, N., Hales, B., Chan, F., Hill, T. M., Gaylord, B., Sanford, E., Byrne, R. H., Sabine, C. L., Greeley, D., and Juranek, L.: Chemical and biological impacts of ocean acidification along the west coast of North America, *Estuar. Coast. Shelf Sci.*, 183, 260–270, <https://doi.org/10.1016/j.ecss.2016.08.043>, 2016.
- 615 Field, J. C. and Francis, R. C.: Considering ecosystem-based fisheries management in the California Current, *Mar. Policy*, 30, 552–569, <https://doi.org/10.1016/j.marpol.2005.07.004>, 2006.
- Frölicher, T. L. and Laufkötter, C.: Emerging risks from marine heat waves, *Nat. Commun.*, 9, 650, <https://doi.org/10.1038/s41467-018-03163-6>, 2018.
- Fumo, J. T., Carter, M. L., Flick, R. E., Rasmussen, L. L., Rudnick, D. L., and Iacobellis, S. F.: Contextualizing marine heatwaves in the Southern California Bight under anthropogenic climate change, *J. Geophys. Res. Oceans*, 125, <https://doi.org/10.1029/2019JC015674>, 2020.
- 620 García-Reyes, M. and Largier, J.: Observations of increased wind-driven coastal upwelling off central California, *J. Geophys. Res. Oceans*, 115, <https://doi.org/10.1029/2009JC005576>, 2010.
- García-Reyes, M. and Largier, J. L.: Seasonality of coastal upwelling off central and northern California: New insights, including temporal and spatial variability, *J. Geophys. Res. Oceans*, 117, <https://doi.org/10.1029/2011JC007629>, 2012.
- 625



- Gattuso, J.-P., Epitalon, J.-M., Lavigne, H., and Orr, J.: seacarb: seawater carbonate chemistry. R package version 3.2.10., 2018.
- Gentemann, C. L., Fewings, M. R., and García-Reyes, M.: Satellite sea surface temperatures along the West Coast of the United States during the 2014–2016 northeast Pacific marine heat wave, *Geophys. Res. Lett.*, 44, 312–319, 630 <https://doi.org/10.1002/2016GL071039>, 2017.
- Gobler, C. J. and Baumann, H.: Hypoxia and acidification in ocean ecosystems: coupled dynamics and effects on marine life, *Biol. Lett.*, 12, 20150976, <https://doi.org/10.1098/rsbl.2015.0976>, 2016.
- Grantham, B. A., Chan, F., Nielsen, K. J., Fox, D. S., Barth, J. A., Huyer, A., Lubchenco, J., and Menge, B. A.: Upwelling-driven nearshore hypoxia signals ecosystem and oceanographic changes in the northeast Pacific, *Nature*, 429, 749–754, 635 <https://doi.org/10.1038/nature02605>, 2004.
- Gruber, N., Hauri, C., Lachkar, Z., Loher, D., Frölicher, T. L., and Plattner, G.-K.: Rapid progression of ocean acidification in the California Current System, *Science*, 337, 220–223, <https://doi.org/10.1126/science.1216773>, 2012.
- Hales, B., Chipman, D., and Takahashi, T.: High-frequency measurement of partial pressure and total concentration of carbon dioxide in seawater using microporous hydrophobic membrane contactors, *Limnol. Oceanogr. Methods*, 2, 356–364, 640 <https://doi.org/10.4319/lom.2004.2.356>, 2004.
- Hauri, C., Gruber, N., Vogt, M., Doney, S. C., Feely, R. A., Lachkar, Z., Leinweber, A., McDonnell, A. M. P., Munnich, M., and Plattner, G.-K.: Spatiotemporal variability and long-term trends of ocean acidification in the California Current System, *Biogeosciences*, 10, 193–216, <https://doi.org/10.5194/bg-10-193-2013>, 2013.
- Hickey, B. M.: The California current system—hypotheses and facts, *Prog. Oceanogr.*, 8, 191–279, 645 [https://doi.org/10.1016/0079-6611\(79\)90002-8](https://doi.org/10.1016/0079-6611(79)90002-8), 1979.
- Hodgson, E. E., Kaplan, I. C., Marshall, K. N., Leonard, J., Essington, T. E., Busch, D. S., Fulton, E. A., Harvey, C. J., Hermann, A. J., and McElhany, P.: Consequences of spatially variable ocean acidification in the California Current: Lower pH drives strongest declines in benthic species in southern regions while greatest economic impacts occur in northern regions, *Ecol. Modell.*, 383, 106–117, <https://doi.org/10.1016/j.ecolmodel.2018.05.018>, 2018.
- 650 Hofmann, A. F., Peltzer, E. T., Walz, P. M., and Brewer, P. G.: Hypoxia by degrees: Establishing definitions for a changing ocean, *Deep Sea Res. Part I: Oceanographic Research Papers*, 58, 1212–1226, <https://doi.org/10.1016/j.dsr.2011.09.004>, 2011a.
- Hofmann, G. E., Smith, J. E., Johnson, K. S., Send, U., Levin, L. A., Micheli, F., Paytan, A., Price, N. N., Peterson, B., Takeshita, Y., Matson, P. G., Crook, E. D., Kroeker, K. J., Gambi, M. C., Rivest, E. B., Frieder, C. A., Yu, P. C., and Martz, 655 T. R.: High-Frequency dynamics of ocean pH: A multi-ecosystem comparison, *PLoS One*, 6, e28983, <https://doi.org/10.1371/journal.pone.0028983>, 2011b.
- Hollarsmith, J. A., Sadowski, J. S., Picard, M. M. M., Cheng, B., Farlin, J., Russell, A., and Grosholz, E. D.: Effects of seasonal upwelling and runoff on water chemistry and growth and survival of native and commercial oysters, *Limnol. Oceanogr.*, 65, 224–235, <https://doi.org/10.1002/lno.11293>, 2020.



- 660 Howard, E. M., Penn, J. L., Frenzel, H., Seibel, B. A., Bianchi, D., Renault, L., Kessouri, F., Sutula, M. A., McWilliams, J. C., and Deutsch, C.: Climate-driven aerobic habitat loss in the California Current System, *Sci. Adv.*, 6, eaay3188, <https://doi.org/10.1126/sciadv.aay3188>, 2020.
- Huyer, A.: Coastal upwelling in the California current system, *Prog. Oceanogr.*, 12, 259–284, [https://doi.org/10.1016/0079-6611\(83\)90010-1](https://doi.org/10.1016/0079-6611(83)90010-1), 1983.
- 665 IPCC: IPCC special report on the ocean and cryosphere in a changing climate, 1st ed., edited by: Pörtner, H.-O., Roberts, D. C., Masson-Delmotte, V., Zhai, P., Tignor, M., Poloczanska, E., Mintenbeck, K., Alegria, A., Nicolai, M., Okem, A., Petzold, J., Rama, B., and Weyer, N. M., Cambridge University Press, Cambridge, UK and New York, NY, USA, 755 pp., <https://doi.org/10.1017/9781009157964>, 2019.
- Jacox, M. G., Hazen, E. L., Zaba, K. D., Rudnick, D. L., Edwards, C. A., Moore, A. M., and Bograd, S. J.: Impacts of the 670 2015–2016 El Niño on the California Current System: Early assessment and comparison to past events, *Geophys. Res. Lett.*, 43, 7072–7080, <https://doi.org/10.1002/2016GL069716>, 2016.
- Jacox, M. G., Edwards, C. A., Hazen, E. L., and Bograd, S. J.: Coastal upwelling revisited: Ekman, Bakun, and improved upwelling indices for the U.S. West Coast, *J. Geophys. Res. Oceans*, 123, 7332–7350, <https://doi.org/10.1029/2018JC014187>, 2018.
- 675 Kekuewa, S. A. H., Courtney, T. A., Cyronak, T., and Andersson, A. J.: Seasonal nearshore ocean acidification and deoxygenation in the Southern California Bight, *Sci. Rep.*, 12, 17969, <https://doi.org/10.1038/s41598-022-21831-y>, 2022.
- Kelly, M. W. and Hofmann, G. E.: Adaptation and the physiology of ocean acidification, *Funct. Ecol.*, 27, 980–990, <https://doi.org/10.1111/j.1365-2435.2012.02061.x>, 2013.
- Kroeker, K. J., Kordas, R. L., Crim, R., Hendriks, I. E., Ramajo, L., Singh, G. S., Duarte, C. M., and Gattuso, J.-P.: Impacts 680 of ocean acidification on marine organisms: quantifying sensitivities and interaction with warming, *Glob. Change Biol.*, 19, 1884–1896, <https://doi.org/10.1111/gcb.12179>, 2013.
- Kennedy, E. G., Zulian, M., Hamilton, S. L., Hill, T. M., Delgado, M., Fish, C. R., Gaylord, B., Kroeker, K. J., Palmer, H. M., Ricart, A. M., Sanford, E., Spalding, A. K., Ward, M. A., Carrasco, G., Elliott, M., Grisby, G. V., Harris, E., Jahneke, J., Rocheleau, C. N., Westerink, S., Wilmot, M. I.: Multistressor Observations of Coastal Hypoxia and Acidification (MOCHA) 685 Synthesis (NCEI Accession 0277984), NOAA National Centers for Environmental Information [data set], <https://doi.org/10.25921/2vve-fh39>, 2023.
- Kroeker, K. J., Donham, E. M., Vylet, K., Warren, J. K., Cheresh, J., Fiechter, J., Freiwald, J., and Takeshita, Y.: Exposure to extremes in multiple global change drivers: Characterizing pH, dissolved oxygen, and temperature variability in a dynamic, upwelling dominated ecosystem, *Limnol. Oceanogr.*, 1–13, <https://doi.org/10.1002/lno.12371>, 2023.
- 690 Lai, C.-Z., DeGrandpre, M. D., and Darlington, R. C.: Autonomous optofluidic chemical analyzers for marine applications: Insights from the Submersible Autonomous Moored Instruments (SAMI) for pH and pCO₂, *Front. Mar. Sci.*, 4, 2018.
- Low, N. H. N., Micheli, F., Aguilar, J. D., Arce, D. R., Boch, C. A., Bonilla, J. C., Bracamontes, M. Á., De Leo, G., Diaz, E., Enríquez, E., Hernandez, A., Martinez, R., Mendoza, R., Miranda, C., Monismith, S., Ramade, M., Rogers-Bennett, L.,



- Romero, A., Salinas, C., Smith, A. E., Torre, J., Villavicencio, G., and Woodson, C. B.: Variable coastal hypoxia exposure and drivers across the southern California Current, *Sci. Rep.*, 11, 10929, <https://doi.org/10.1038/s41598-021-89928-4>, 2021.
- Marchesiello, P., McWilliams, J. C., and Shepetchkin, A.: Equilibrium structure and dynamics of the California Current System, *J. Phys. Oceanogr.*, 33, 753–783, [https://doi.org/10.1175/1520-0485\(2003\)33<753:ESADOT>2.0.CO;2](https://doi.org/10.1175/1520-0485(2003)33<753:ESADOT>2.0.CO;2), 2003.
- Marshall, K. N., Kaplan, I. C., Hodgson, E. E., Hermann, A., Busch, D. S., McElhany, P., Essington, T. E., Harvey, C. J., and Fulton, E. A.: Risks of ocean acidification in the California Current food web and fisheries: ecosystem model projections, *Glob. Change Biol.*, 23, 1525–1539, <https://doi.org/10.1111/gcb.13594>, 2017.
- Martz, T. R., Connery, J. G., and Johnson, K. S.: Testing the Honeywell Durafet® for seawater pH applications, *Limnol. Oceanogr. Methods*, 8, 172–184, <https://doi.org/10.4319/lom.2010.8.172>, 2010.
- Martz, T. R., Daly, K. L., Byrne, R. H., Stillman, J. H., and Turk, D.: Technology for ocean acidification research: Needs and availability, *Oceanography*, 28, 40–47, 2015.
- Middelburg, J. J., Soetaert, K., and Hagens, M.: Ocean alkalinity, buffering and biogeochemical processes, *Rev. Geophys.*, 58, e2019RG000681, <https://doi.org/10.1029/2019RG000681>, 2020.
- Ricart, A. M., Ward, M., Hill, T. M., Sanford, E., Kroeker, K. J., Takeshita, Y., Merolla, S., Shukla, P., Ninokawa, A. T., Elsmore, K., and Gaylord, B.: Coast-wide evidence of low pH amelioration by seagrass ecosystems, *Glob. Change Biol.*, 27, 2580–2591, <https://doi.org/10.1111/gcb.15594>, 2021.
- Risien, C. M., Fewings, M. R., Fisher, J. L., Peterson, J. O., and Morgan, C. A.: Spatially gridded cross-shelf hydrographic sections and monthly climatologies from shipboard survey data collected along the Newport Hydrographic Line, 1997–2021, *Data Brief*, 41, 107922, <https://doi.org/10.1016/j.dib.2022.107922>, 2022.
- Rogers-Bennett, L. and Catton, C. A.: Marine heat wave and multiple stressors tip bull kelp forest to sea urchin barrens, *Sci. Rep.*, 9, 15050, <https://doi.org/10.1038/s41598-019-51114-y>, 2019.
- Rosenau, N. A., Galavotti, H., Yates, K. K., Bohlen, C. C., Hunt, C. W., Liebman, M., Brown, C. A., Pacella, S. R., Largier, J. L., Nielsen, K. J., Hu, X., McCutcheon, M. R., Vasslides, J. M., Poach, M., Ford, T., Johnston, K., and Steele, A.: Integrating high-resolution coastal acidification monitoring data across seven United States estuaries, *Front. Mar. Sci.*, 8, 2021.
- Ruhl, H. A., Brown, J. A., Harper, A. R., Hazen, E. L., deWitt, L., Daniel, P., DeVogelaere, A., Kudela, R. M., Ryan, J. P., Fischer, A. D., Muller-Karger, F. E., and Chavez, F. P.: Integrating biodiversity and environmental observations: In support of National Marine Sanctuary and Large Marine Ecosystem assessments, *Oceanography*, 34, 142–155, 2021.
- Sakuma, K.: Project report: Rockfish Recruitment and Ecosystem Assessment (NOAA Ship Reuben Lasker, RL-22-02, April 28 - June 16, 2022), NMFS Southwest Fisheries Science Center, Santa Cruz, CA, 2022.
- Salop, P. and Herrmann, C.: 2019 RMP Water cruise report, Regional Monitoring Program for Water Quality in San Francisco Bay, San Francisco Estuary Institute, Richmond, CA, 2019.
- Sanford, E. and Kelly, M. W.: Local adaptation in marine invertebrates, *Ann. Rev. Mar. Sci.*, 3, 509–535, <https://doi.org/10.1146/annurev-marine-120709-142756>, 2011.



- Sanford, E., Sones, J. L., García-Reyes, M., Goddard, J. H. R., and Largier, J. L.: Widespread shifts in the coastal biota of northern California during the 2014–2016 marine heatwaves, *Sci. Rep.*, 9, 4216, <https://doi.org/10.1038/s41598-019-40784-3>, 2019.
- Schar, D., Atkinson, M., Johengen, T., Pinchuk, A., Purcell, H., Robertson, C., Smith, G. J., and Tamburri, M.: Performance demonstration statement: Sunburst Sensors SAMI-CO₂, Alliance for Coastal Technologies, Chesapeake Biological Laboratory, Solomons, Maryland, USA, 2009.
- Sharp, J. D., Fassbender, A. J., Carter, B. R., Lavin, P. D., and Sutton, A. J.: A monthly surface pCO₂ product for the California Current Large Marine Ecosystem, *Earth Syst. Sci. Data*, 14, 2081–2108, <https://doi.org/10.5194/essd-14-2081-2022>, 2022.
- Siedlecki, S., Bjorkstedt, E., Feely, R., Sutton, A., Cross, J., and Newton, J.: Impact of the Blob on the Northeast Pacific Ocean biogeochemistry and ecosystems, *US Clivar Variations*, 14, 2016.
- Siedlecki, S. A., Pilcher, D., Howard, E. M., Deutsch, C., MacCreedy, P., Norton, E. L., Frenzel, H., Newton, J., Feely, R. A., Alin, S. R., and Klinger, T.: Coastal processes modify projections of some climate-driven stressors in the California Current System, *Biogeosciences*, 18, 2871–2890, <https://doi.org/10.5194/bg-18-2871-2021>, 2021.
- Sunday, J. M., Howard, E., Siedlecki, S., Pilcher, D. J., Deutsch, C., MacCreedy, P., Newton, J., and Klinger, T.: Biological sensitivities to high-resolution climate change projections in the California Current marine ecosystem, *Glob. Change Biol.*, 1–15, <https://doi.org/10.1111/gcb.16317>, 2021.
- Swiney, K. M., Long, W. C., Foy, R. J., Fields, D. M.: Decreased pH and increased temperatures affect young-of-the-year red king crab (*Paralithodes camtschaticus*), *ICES J. Mar. Sci.*, 74, 1191–1200, <https://doi.org/10.1093/icesjms/fsw251>, 2017.
- Sydeman, W. J., Thompson, S. A., García-Reyes, M., Kahru, M., Peterson, W. T., and Largier, J. L.: Multivariate ocean-climate indicators (MOCI) for the central California Current: Environmental change, 1990–2010, *Prog. Oceanogr.*, 120, 352–369, <https://doi.org/10.1016/j.pocean.2013.10.017>, 2014.
- Taylor-Burns, R., Cochran, C., Ferron, K., Harris, M., Thomas, C., Fredston, A., and Kendall, B. E.: Locating gaps in the California Current System ocean acidification monitoring network, *Sci. Prog.*, 103, 0036850420936204, <https://doi.org/10.1177/0036850420936204>, 2020.
- Terrill, E., Peck, S., Hazard, L., Davis, R. E., DiGiacomo, P. M., Jones, B. H., Keen, C., Moline, M., Orcutt, J., Stolzenbach, K., Washburn, L., Helling, H., Long, J., Magdziarz, S., Laughlin, M., and Kasschau, J.: The Southern California Coastal Ocean Observing System, *Oceans 2006*, 1–8, <https://doi.org/10.1109/OCEANS.2006.306877>, 2006.
- Trowbridge, J., Weller, R., Kelley, D., Dever, E., Plueddemann, A., Barth, J. A., and Kawka, O.: The Ocean Observatories Initiative, *Front. Mar. Sci.*, 6, 2019.
- Wang, D., Gouhier, T. C., Menge, B. A., and Ganguly, A. R.: Intensification and spatial homogenization of coastal upwelling under climate change, *Nature*, 518, 390–394, <https://doi.org/10.1038/nature14235>, 2015.



- 760 Ward, M., Spalding, A. K., Levine, A., and Wolters, E. A.: California shellfish farmers: Perceptions of changing ocean conditions and strategies for adaptive capacity, *Ocean Coast Manag.*, 225, 106155, <https://doi.org/10.1016/j.ocecoaman.2022.106155>, 2022.
- Weisberg, S., Chan, F., Barry, J., Boehm, A., NOAA, S. B., Cooley, S., Feely, R., Levin, L., Carter, H., Abderrahim, M., and Kimball, J.: Enhancing California's ocean acidification and hypoxia monitoring network: Recommendations to the Ocean
765 Protection Council from the California Ocean Acidification and Hypoxia Science Task Force, California Ocean Science Trust, Sacramento, California, USA, 2020.
- Wilkinson, M. D., Dumontier, M., Aalbersberg, Ij. J., Appleton, G., Axton, M., Baak, A., Blomberg, N., Boiten, J.-W., da Silva Santos, L. B., Bourne, P. E., Bouwman, J., Brookes, A. J., Clark, T., Crosas, M., Dillo, I., Dumon, O., Edmunds, S., Evelo, C. T., Finkers, R., Gonzalez-Beltran, A., Gray, A. J. G., Groth, P., Goble, C., Grethe, J. S., Heringa, J., 't Hoen, P. A.
770 C., Hooft, R., Kuhn, T., Kok, R., Kok, J., Lusher, S. J., Martone, M. E., Mons, A., Packer, A. L., Persson, B., Rocca-Serra, P., Roos, M., van Schaik, R., Sansone, S.-A., Schultes, E., Sengstag, T., Slater, T., Strawn, G., Swertz, M. A., Thompson, M., van der Lei, J., van Mulligen, E., Velterop, J., Waagmeester, A., Wittenburg, P., Wolstencroft, K., Zhao, J., and Mons, B.: The FAIR Guiding Principles for scientific data management and stewardship, *Sci. Data*, 3, 160018, <https://doi.org/10.1038/sdata.2016.18>, 2016.
- 775 Woodson, C. B., Micheli, F., Boch, C., Al-Najjar, M., Espinoza, A., Hernandez, A., Vázquez-Vera, L., Saenz-Arroyo, A., Monismith, S. G., and Torre, J.: Harnessing marine microclimates for climate change adaptation and marine conservation, *Conserv. Lett.*, 12, e12609, <https://doi.org/10.1111/conl.12609>, 2019.